

# A Comprehensive Review of Domain Adaptation Techniques for Agricultural Image Analysis in Precision Agriculture

Xing Hu<sup>a,\*\*</sup>, Siyuan Chen<sup>a</sup>, Xuming Huang<sup>b</sup>, Qianqian Duan<sup>c</sup>, Huiliang Shang<sup>d,\*</sup> and Dawei Zhang<sup>a,\*</sup>

<sup>a</sup>School of Optical-Electrical and Computer Engineering, University of Shanghai for Science and Technology, No. 516, Jungong Road, Shanghai, 200093, China

<sup>b</sup>Department of Computer Sciences, University of Wisconsin-Madison, 1210 W Dayton Street, Madison, WI, 53706, USA

<sup>c</sup>School of Electronics and Electrical Engineering, Shanghai University of Engineering Science, Shanghai, 201620, China

<sup>d</sup>Future Information Innovation Institute, Fudan University, Shanghai, China

## ARTICLE INFO

### Keywords:

Domain Adaptation, Deep Learning, Agricultural Image Analysis, Cross-Domain Transfer, Adversarial Learning

## ABSTRACT

With the growing application of computer vision in agriculture, image analysis has become essential for tasks such as crop health monitoring and pest detection. However, significant domain shifts caused by environmental variations, different crop types, and diverse data acquisition methods hinder model generalization across regions, seasons, and complex agricultural settings. This paper investigates how Domain Adaptation (DA) techniques can address these challenges by improving cross-domain transferability in agricultural image analysis. Given the limited availability of labeled data, weak model adaptability, and dynamic field conditions, DA has emerged as a promising solution. The review systematically summarizes recent advances in DA for agricultural imagery, focusing on applications such as crop health monitoring, pest detection, and fruit recognition, where DA methods have improved performance in diverse domains. DA approaches are categorized into shallow and deep learning methods, including supervised, semi-supervised, and unsupervised strategies, with particular attention to adversarial learning-based techniques that have demonstrated strong potential in complex scenarios. In addition, the paper reviews key public agricultural image datasets, evaluating their strengths and limitations in DA research. In general, this work offers a comprehensive framework and critical insights to guide future research and development of domain adaptation in agricultural vision tasks.

## 1. Introduction

In agricultural image analysis, the high heterogeneity of data acquisition environments and the extreme scarcity of annotated data severely limit the generalizability of models across different application scenarios. Among these challenges, the **domain shift problem**—referring to distribution discrepancies between source and target data—has emerged as a key obstacle hindering the deployment of intelligent agricultural vision systems [1, 2]. To address this issue, **domain adaptation (DA)** techniques have recently gained prominence in agricultural image analysis, aiming to enhance model robustness and transferability across cross-regional, cross-temporal, and cross-device data sources.

Agricultural image data are typically acquired using various sensors (e.g., RGB cameras, near-infrared imagers, hyperspectral sensors) and are highly susceptible to environmental factors such as illumination changes, seasonal cycles, crop varieties, and soil backgrounds. These differences lead to significant distributional shifts for the same task across datasets, causing models trained under conventional paradigms to suffer severe performance degradation when deployed in new environments [3]. For example, models trained on laboratory or demonstration farm data often exhibit sharp accuracy drops when applied to real-world fields, other geographic regions, or different crop growth periods. Domain adaptation extends beyond crops to livestock management, as seen in Dubourvieux et al.’s work on cattle re-identification [4]. Their cumulative multi-domain strategy addresses challenges like varying barn conditions or camera viewpoints, demonstrating DA’s versatility in animal farming.

\*Corresponding author

\*\*Principal corresponding author

 242250440@st.usst.edu.cn (S. Chen); xhuang546@wisc.edu (X. Huang); dqq1019@163.com (Q. Duan)

 huxing@usst.edu.cn (X. Hu); shanghl@fudan.edu.cn (H. Shang); dwzhang@usst.edu.cn (D. Zhang)

ORCID(s): 0000-0003-1930-0372 (X. Hu)

Furthermore, annotating agricultural images generally requires expert knowledge from agronomists and plant protection specialists, resulting in high annotation costs and limited data scalability. Compared to general computer vision tasks, the availability of high-quality labeled datasets in agriculture remains extremely limited [5]. Consequently, directly transferring pre-trained models from natural image domains proves ineffective, highlighting the necessity of DA techniques to reduce annotation dependency and improve cross-domain adaptability. The core objective of DA is to minimize feature distribution discrepancies between the source and target domains, enabling models to perform comparably in the target domain.

In recent years, DA has shown significant promise in key agricultural applications such as crop disease and pest detection, hyperspectral image analysis, crop growth monitoring, and precision farming management. Particularly under unsupervised or weakly supervised settings, the ability of DA to model distributional shifts makes it a vital enabler of scalable agricultural visual intelligence. While numerous reviews on transfer learning and domain adaptation exist in the field of natural image analysis [6, 7, 8, 9, 10, 11, 12, 13, 14, 15, 16, 17], systematic reviews specifically focused on agricultural image analysis remain limited.

To address this gap, this review systematically summarizes the current landscape of domain adaptation methods in agricultural image analysis. We categorize existing approaches into two major classes—shallow and deep learning models—and examine their respective supervised, semi-supervised, and unsupervised strategies. Particular emphasis is placed on adversarial learning-based adaptation methods and their effectiveness in addressing key challenges such as seasonal variation, multi-source data fusion, and annotation scarcity. This review ultimately serves as a methodological reference for the development of next-generation intelligent agricultural systems.

## 2. Background

### 2.1. Domain Shift in Agricultural Image Analysis

In agricultural image analysis, **domain shift** refers to the discrepancy in data distribution between the training dataset (source domain) and the test dataset (target domain). This shift can cause models to perform well on the source domain but fail to generalize effectively to the target domain, thereby significantly degrading overall performance. Agricultural images often exhibit substantial distributional differences due to various factors, including environmental conditions, crop types, and imaging configurations. Specifically, images captured in different geographic regions or under varying environmental settings—such as changes in lighting, climate, seasonal dynamics, crop varieties, and sensor viewpoints—can exacerbate domain shift, presenting serious challenges to model transferability.

As shown in Figure 1, numerous studies have explored the use of domain adaptation (DA) techniques to address these challenges in agricultural vision tasks. DA methods aim to mitigate domain shift by aligning feature distributions between the source and target domains, enabling more robust and generalizable performance.

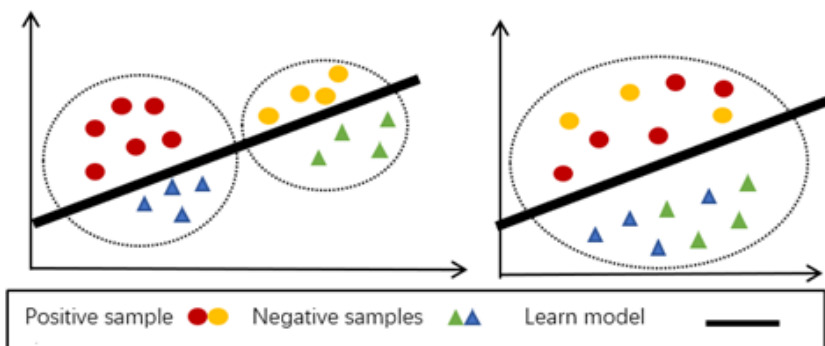


**Figure 1:** Illustration of source and target data: (left) misaligned feature distribution due to domain shift; (right) improved alignment after applying domain adaptation.

For example, in crop classification tasks, images collected from different regions often exhibit marked heterogeneity in appearance. Figure 2 illustrates this phenomenon using aerial scenes from Ghaziabad, India, captured during the rainy and dry seasons. The images clearly reflect environmental differences, such as lighting and climate,

which introduce significant distributional discrepancies. These shifts can impact the accuracy and robustness of key agricultural vision tasks, including crop monitoring and pest detection—especially in cross-regional, cross-seasonal, and cross-device scenarios.

As the demand for scalable agricultural image analysis continues to grow, domain adaptation has emerged as a critical technology for improving cross-domain generalization. By reducing distributional gaps between domains, DA techniques enhance the reliability of agricultural models across diverse settings, ultimately supporting more accurate, consistent, and transferable performance in real-world applications.



**Figure 2:** Aerial scenes from Ghaziabad, India, captured during rainy and dry seasons, illustrating domain shift due to seasonal variation.

## 2.2. Domain Adaptation and Transfer Learning

In a typical transfer learning (TL) framework, two fundamental concepts are involved: *domain* and *task*. A domain refers to a specific feature space along with its marginal probability distribution, while a task is defined by a label space and an associated predictive function. The goal of TL is to leverage knowledge learned from a source task  $T_A$  in domain  $A$  and apply it to a target task  $T_B$  in domain  $B$ . Notably, either the domain, the task, or both may differ between the source and target settings.

*Domain Adaptation* (DA) is a specialized and widely studied subfield of TL. In DA, the feature space and task remain consistent across domains, but the marginal distributions differ, i.e.,  $P_S(X) \neq P_T(X)$ . Formally, let  $X \times Y$  denote the joint feature and label space. The source domain  $S$  and target domain  $T$  are defined over this space, but their respective distributions  $P_S$  and  $P_T$  differ. Assume there are  $n_S$  labeled samples in the source domain,  $D_S = \{(x_i^S, y_i^S)\}_{i=1}^{n_S}$ , and  $n_T$  samples (either labeled or unlabeled) in the target domain,  $D_T = \{x_j^T\}_{j=1}^{n_T}$ .

The objective of domain adaptation is to transfer knowledge from the source domain  $S$  to improve model performance on the target domain  $T$  for a shared task. This is typically achieved by aligning the distributions of the two domains—either explicitly or implicitly—through various adaptation strategies.

### 2.3. Domain Adaptation Problem Setup

In the agricultural domain, domain adaptation methods face unique challenges stemming from pronounced discrepancies between source and target domains. These discrepancies are particularly evident in three dimensions: spatial distribution, temporal sequences, and modality diversity. Agricultural image data are typically collected from heterogeneous platforms, including satellite remote sensing, unmanned aerial vehicles (UAVs), and ground-based sensors. Due to variations in climate conditions, crop types, and sensor characteristics across different environments, substantial distributional heterogeneity arises. To address this, DA techniques have become essential for enhancing generalization by bridging distribution gaps across domains.

Depending on the availability of labeled data in the target domain, DA methods are commonly categorized into supervised, semi-supervised, and unsupervised approaches. Among them, unsupervised domain adaptation (UDA) is especially critical in agriculture due to the scarcity and cost of annotations.

Early efforts in DA primarily focused on aligning data distributions between source and target domains through three main pathways: instance-based alignment (e.g., sample reweighting), feature space transformation (e.g., subspace learning), and classifier parameter adaptation. These traditional approaches typically rely on hand-crafted features and statistical alignment techniques to reduce domain discrepancy. For instance, instance-based approaches adjust the contribution of each source sample to better match the target distribution; feature-based methods seek a shared subspace through linear projections; and classifier-based methods improve cross-domain performance by regularizing classifier parameters. These methods, collectively referred to as **shallow domain adaptation (Shallow DA)**, offer advantages such as low computational complexity, high efficiency, and strong interpretability—making them suitable for resource-constrained agricultural applications.

The emergence of deep learning has significantly reshaped the DA landscape. In 2014, Girshick et al. [18] introduced the Region-based Convolutional Neural Network (R-CNN), pioneering CNNs for object detection. Fast R-CNN [19] and Faster R-CNN [20] further improved this framework by integrating region proposal, feature extraction, and classification into an end-to-end pipeline. In agriculture, Fuentes et al. [21] applied Faster R-CNN with VGGNet/ResNet backbones to detect and localize tomato diseases and pests, achieving a mean Average Precision (mAP) of 85.98% across 10 classes. This success exemplifies the widespread adoption of **deep domain adaptation (Deep DA)** in agricultural image analysis.

In summary, DA methods in agriculture can be categorized into two paradigms: shallow and deep adaptation. Shallow DA includes classical techniques based on instance reweighting, feature alignment, and classifier adjustment, while Deep DA encompasses modern methods leveraging deep neural networks. These can be further classified into supervised, semi-supervised, and unsupervised approaches depending on label availability, as summarized in Table 1. Each paradigm offers complementary strengths in terms of computational efficiency, scalability, and generalization.

## 3. Shallow DA Methods

This section reviews shallow domain adaptation (DA) methods that rely on manually engineered features and traditional machine learning algorithms in the context of agricultural data analysis. These methods are typically categorized into three main strategies: (1) instance weighting, (2) feature transformation, and (3) classifier-based adaptation.

### 3.1. Instance Weighting

Instance weighting is a widely adopted strategy in shallow DA, particularly in agricultural image analysis. These methods aim to adjust the marginal distributions of the source and target samples to reduce domain discrepancies. Let  $p_t(x)$  and  $p_s(x)$  denote the marginal density functions of the target and source samples, respectively. The importance weight  $w(x)$  is defined as:

$$w(x) = \frac{p_t(x)}{p_s(x)} \quad (1)$$

**Table 1**

Taxonomy of Domain Adaptation Methods in Agricultural Image Analysis

CATEGORY	SUBCATEGORIES	TYPICAL EXAMPLES
Shallow DA	Instance-based	DIAFAN-TL, RHM, HSI, CSSPL
	Feature-based	SA, TSSA, ECMDCM, CropSTGAN, MultiCropGAN, Spatial-Invariant Features, RKHS Features, Sensor-driven Hierarchical DA, PSO-TrAdaBoost, ESSL, HSL-GM
	Classifier-based	MLCA, BCC, SSGF, MDAF, WRF, CDELM, BHC, DASVM, SD-AL, AMKFL, VSV, EasyTL
Deep DA	Semi-supervised	MAML, WheatSeedBelt, SSDA-WheatHead, SSDA-WheatSeg, TDA-YOLO, SCDAL, CDADA
	Unsupervised	MSFF, GAN-DA, DeepDA-Net, U-DA-Net, TriADA, MaxEnt-DA, DAE-DANN, Self-Attn-DA, ADANN, OpenDA, AdaptSeg-Net, ADVENT, BDL, DFENet, TSAN, DAN, WDGR, CORAL, Transformer-UDA, MRAN, WPS-DSA, NCADA, TCANet, DDA-Net, TDDA, TST-Net, AMF-FSL, MSUN, MSCN, AMRAN, DJ-DANs, CLA

In this approach, source domain samples are weighted according to their similarity or relevance to target domain samples. For example, crop observation data from geographically adjacent regions might be assigned higher weights to better reflect the target domain distribution. Training a model—such as a classifier or regressor—on these reweighted samples can significantly mitigate the distributional gap between domains. As illustrated in Figure 3, instance weighting visibly reduces the divergence between source and target domains.

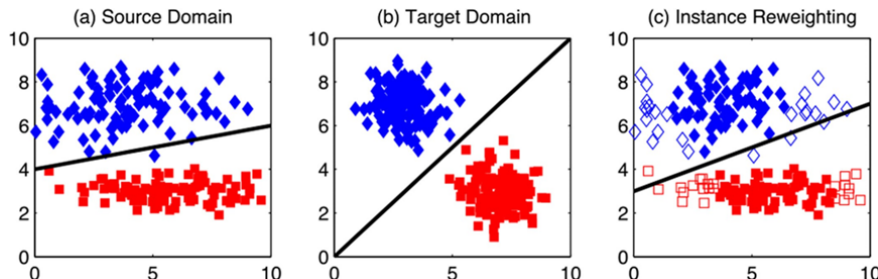


**Figure 3:** Instance weighting to alleviate domain shift. (a) Source domain after feature matching. (b) Target domain after feature matching. (c) Source domain with joint feature matching and instance weighting, where unfilled markers indicate less relevant, low-weight instances. Image adapted from Longet et al. [22].

Molina-Cabanillas et al. [23] introduced DIAFAN-TL (Domain-Invariant Agricultural Features Adaptation Network for Transfer Learning), an instance-weighted learning algorithm for phenological prediction in olive tree cultivars. This method dynamically assigns weights to training samples based on inter-domain relevance, thereby enhancing information diversity while reducing sample inconsistency. Yaras et al. [24] proposed Random Histogram Matching (RHM), which leverages data augmentation to improve satellite image domain adaptation. By modeling sensor differences and environmental variations as nonlinear pixel transformations and applying deep neural networks for augmentation, this method improves robustness to domain shifts.

To further optimize the framework, Cui et al. [25] developed the Iterative Weighted Active Transfer Learning (IWATL) approach for hyperspectral image (HSI) classification. Through a dual-evaluation mechanism, it adaptively updates source sample weights, significantly enhancing classification performance. Li et al. [26] proposed the Cost-Sensitive Self-Paced Learning (CSSPL) framework, which integrates hybrid weight regularization for selecting multi-temporal samples, addressing seasonal and temporal variances in agricultural monitoring.

In summary, instance-based shallow DA methods typically follow a two-stage optimization process: (1) adjusting the sample distribution via reweighting or selection, and (2) integrating the adapted data into a robust classifier. These compound strategies are particularly effective in agricultural remote sensing, where data heterogeneity is prevalent, and have demonstrated clear improvements in transferability and generalization.

### 3.2. Feature Transformation

Feature-based domain adaptation methods aim to map data from the source and target domains into a shared, domain-invariant feature representation space. This is typically achieved through techniques such as subspace alignment, manifold learning, and low-rank representation. The primary objective is to reduce the distributional discrepancy between domains during the process of joint feature extraction [27].

As illustrated in Figure 4, these methods first construct a common feature space that captures domain-invariant properties. A classifier is then trained using the transformed source domain features and corresponding labels, enabling more accurate predictions for target domain samples. Implementation strategies generally fall into two categories: subspace-based projection reconstruction and nonlinear transformation-based feature re-encoding.

The overarching goal is to align the statistical properties of features across domains by transforming the feature space, thereby enhancing the model's generalization ability in the target domain. This approach is particularly effective in agricultural scenarios characterized by domain shifts induced by seasonal, geographical, or sensor-based variations.

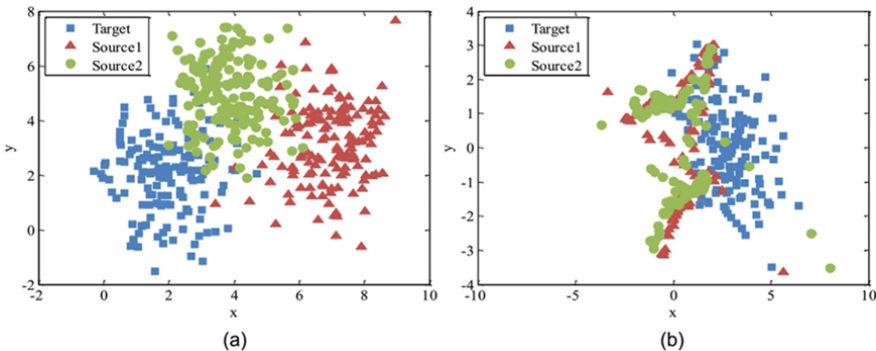


**Figure 4:** Feature transformation for domain adaptation. Each color represents a distinct domain. (a) Feature distributions of two source domains and one target domain before transformation. (b) Aligned feature distributions after transformation. Image adapted from Wang et al. [28].

#### 3.2.1. Subspace-Based Adaptation

Subspace-based domain adaptation (DA) methods typically project source and target samples into separate subspaces using subspace learning or dimensionality reduction techniques, and then align the subspaces. The Subspace Alignment (SA) method proposed by Fernando et al. [29] has been extended to multispectral agricultural image classification tasks. By employing Principal Component Analysis (PCA), this method aligns crop spectral feature subspaces across different seasons, alleviating domain shifts caused by lighting and phenological variations. The SA process is illustrated in Figure 5.

As shown, the source domain samples  $X_S \in \mathbb{R}^{n_s \times D}$  contain  $n_s$  samples with  $D$ -dimensional features, and the target domain samples  $X_T \in \mathbb{R}^{n_t \times D}$  share the same dimensionality. PCA is applied to obtain the principal components of the source and target domains, and a linear transformation matrix  $M$  is learned for subspace alignment.

The core formula for subspace alignment is:

$$M = \arg \min_M \| P_s M - P_t \|_F^2 = P_s^T P_t \quad (2)$$

where  $P_s$  and  $P_t$  are the projection matrices (e.g., PCA bases) of the source and target subspaces, respectively, and  $\| \cdot \|_F^2$  denotes the Frobenius norm.

Sun et al. [30] applied SA to cross-view scene classification using Partial Least Squares (PLS) to construct a discriminative subspace shared by both domains, effectively capturing common spectral features across different sensors. They further proposed the Transfer Sparse Subspace Analysis (TSSA) method [31], which incorporates sparse subspace clustering and Maximum Mean Discrepancy (MMD) minimization to retain self-expressive properties of data across maize growth stages. Weilandt et al. [32] introduced the Early Crop Mapping based on Dynamic Clustering Method (ECMDCM), leveraging time-series NDVI and EVI data for improved early-stage crop classification. Li et al. [33] proposed CropSTGAN, which includes a domain mapper to adapt spatial-temporal discrepancies in crop

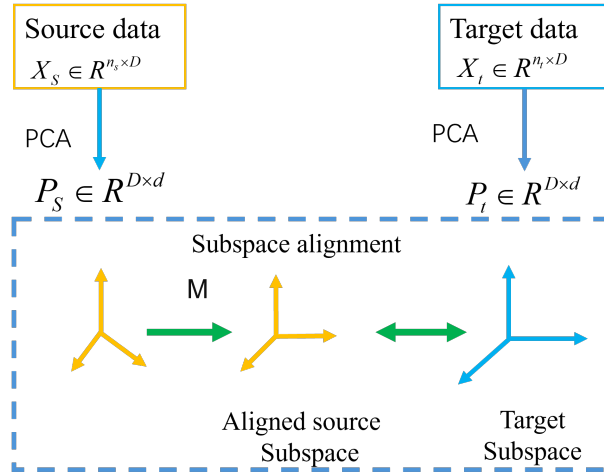


**Figure 5:** Illustration of Subspace Alignment.

mapping, while Wang et al. [34] developed MultiCropGAN, incorporating identity loss to preserve essential features during label space adaptation, with validation in North American farmlands.

Adversarial learning techniques based on category alignment offer another promising avenue. Takahashi et al. [35] proposed a category-guided feature alignment framework, which maps features from both domains into a shared semantic space using adversarial training. Without requiring target domain labels, it leverages source domain categories to enhance domain-invariant learning, thereby improving generalization across crop types and acquisition conditions.

Feature-invariant methods can be viewed as a specific class of subspace adaptation. These methods aim to identify features that remain stable across domains. Bruzzone et al. [36] introduced a multi-objective optimization approach for selecting spatially invariant features to classify non-overlapping scenes, balancing discriminability and spatial robustness. Invariant features may also be extracted in Reproducing Kernel Hilbert Spaces (RKHS) [37]. Paris et al. [38] proposed a sensor-driven hierarchical DA strategy using such features, and Yan et al. [39] introduced a PSO-based TrAdaBoost variant for optimal subspace selection in cross-domain classification.

To address challenges in hyperspectral image classification, such as label-feature inconsistency and computational inefficiency in similarity learning, Yi [40] proposed a subspace learning framework based on set similarity metrics. Compared with traditional methods like Linear Discriminant Analysis (LDA), this approach improves classification accuracy by 8%–15% and reduces training time by 40%–60% on datasets such as Indian Pines and Salinas Valley. Finally, Banerjee [41] proposed a hierarchical subspace alignment method using a semantic-driven binary tree and Grassmannian manifold alignment to address multi-temporal distribution mismatches due to atmospheric, sensor, and labeling differences. It outperforms traditional techniques (e.g., Global GFK, SA) by 5%–6% in accuracy and substantially reduces misclassification in semantically similar crop categories, offering a scalable solution for dynamic agricultural monitoring and environmental analysis.

### 3.2.2. Transformation-Based Adaptation

Transformation-based Domain Adaptation (DA) methods aim to reduce domain discrepancies by directly modifying the distribution of data or features, rather than projecting them into aligned subspaces. These approaches typically apply mapping functions to transform data into a shared representation space or perform direct data-level transformations, thereby aligning the statistical properties of source and target domains.

Aptoula et al. [42] proposed a deep learning-based framework for domain-adaptive classification of crops and weeds, addressing distributional differences caused by variations in lighting, soil properties, and plant phenology. This method embodies the essence of transformation-based DA by projecting agricultural remote sensing data into a new feature space that minimizes both statistical and geometric differences across domains while preserving structural consistency. As illustrated in Figure 6, these methods have shown substantial utility in agricultural remote sensing and crop monitoring applications.

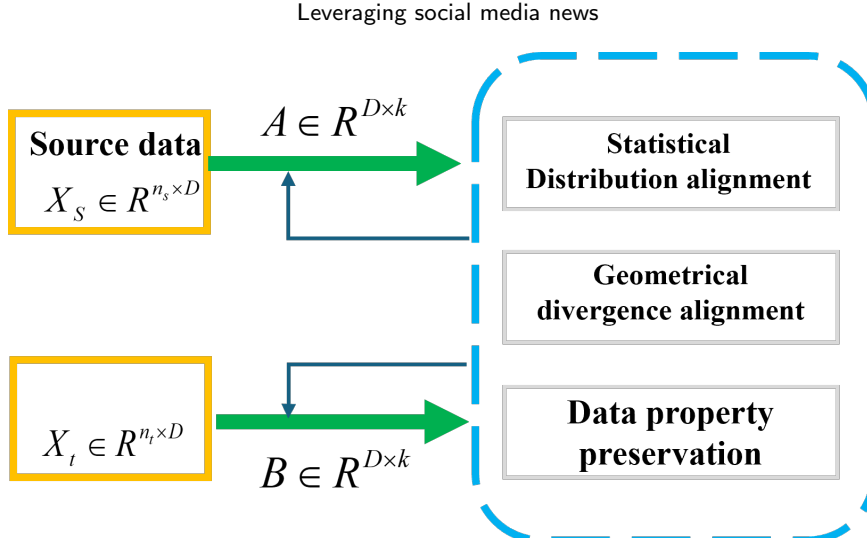


**Figure 6:** Illustration of Transformation-Based Adaptation.

The transformation process typically relies on metrics such as Maximum Mean Discrepancy (MMD), Kullback-Leibler (KL) divergence, or Bregman divergence to quantify inter-domain differences. Among these, MMD is widely favored for agricultural data due to its robustness in high-dimensional settings and is defined as:

$$\text{MMD}(X_s, X_t) = \left\| \frac{1}{n_s} \sum_{\mathbf{x}_i \in X_s} \phi(\mathbf{x}_i) - \frac{1}{n_t} \sum_{\mathbf{x}_j \in X_t} \phi(\mathbf{x}_j) \right\|_F^2 \quad (3)$$

where  $\phi(\cdot)$  denotes the mapping to a Reproducing Kernel Hilbert Space (RKHS), and  $X_s, X_t$  are the source and target domain datasets, respectively.

The effectiveness of different kernel functions in modeling high-dimensional agricultural data (e.g., hyperspectral imagery) lies in their ability to capture nonlinear and complex feature relationships:

- **Linear Kernel:** Suitable for linearly separable data but often inadequate for hyperspectral imagery due to the data's inherent nonlinearity.
- **Radial Basis Function (RBF) Kernel:** Ideal for hyperspectral data as it captures local nonlinear variations across spectral bands, offering a balance between expressiveness and computational efficiency.
- **Polynomial Kernel:** Can model nonlinear feature relationships, especially when inter-band correlations exist; however, high-degree polynomials may incur overfitting and high computational costs.
- **Sigmoid Kernel:** Mimics neural activations but is rarely used in high-dimensional agricultural data due to training instability and poor scalability.

In general, the RBF kernel remains the preferred choice for hyperspectral and other complex agricultural data types due to its robust performance in capturing nonlinear structures. Pan et al. [43] introduced Transfer Component Analysis (TCA), which projects source and target data into a shared RKHS and minimizes domain discrepancy via MMD. The TCA objective function is:

$$\min \text{tr}(W^\top K L K^\top W) + \mu \text{tr}(W^\top W) \quad (4)$$

where  $K$  is the kernel matrix,  $L$  is the MMD matrix,  $W$  is the transformation matrix, and  $\mu$  is the regularization parameter. TCA's adaptability to varied growth stages and its low annotation dependency make it well-suited for tasks such as pest detection, yield estimation, and resource allocation.

Canonical Correlation Analysis (CCA) and its derivatives also provide effective solutions for heterogeneous DA in agricultural contexts. These transformation-based methods, by innovatively modeling domain shifts and tailoring solutions to agricultural data characteristics, contribute significantly to improving model robustness and cross-domain generalization in smart farming systems.

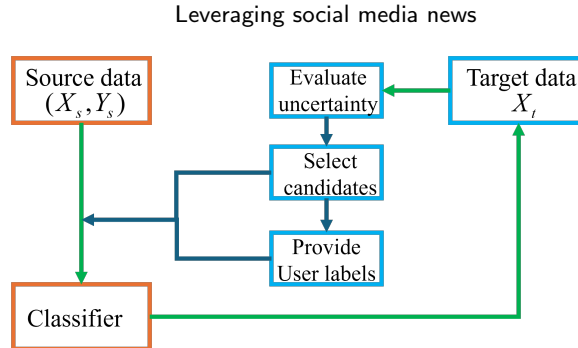


**Figure 7:** Flowchart of an Active Learning (AL) method for domain adaptation.

### 3.3. Classifier-Based Adaptation

Classifier-based domain adaptation (DA) methods refine classifier parameters trained on the source domain by incorporating unlabeled or sparsely labeled samples from the target domain. These approaches have proven particularly valuable in agricultural scenarios characterized by diverse environments, seasonal variability, and limited annotations.

In agriculture, domain shifts often arise due to seasonal changes, varying crop phenotypes, and different imaging conditions. To address these challenges, Bruzzone et al. [44, 45, 46, 47] introduced a maximum likelihood classifier adaptation method that iteratively updates classifier parameters to better reflect the statistical properties of new-season imagery. Similarly, an improved Bayesian cascade classifier [45] enhanced the robustness of cross-regional crop-type recognition. Zhong et al. [48] integrated spectral-spatial guided filtering with adaptive classifier updating, significantly boosting the detection accuracy of crop diseases under heterogeneous field conditions.

Given the complexity of cross-domain agricultural data, ensemble learning has gained traction as an effective strategy to increase robustness. By aggregating predictions from multiple base classifiers, ensemble techniques mitigate overfitting and model bias. Wei et al. [49] proposed a Multi-Domain Adaptation Fusion (MDAF) method that improves farmland classification accuracy across different countries through classifier ensembles, effectively addressing spectral variability.

Weighted classifier transfer approaches—especially those based on Random Forests—are also extensively employed in agriculture. Zhang et al. [50] utilized weighted Random Forests to merge agricultural data from distinct geographic regions, enhancing the performance of cross-regional crop disease detection. Xu et al. [51] extended the Extreme Learning Machine (ELM) framework with kernel alignment to predict crop yields under varying climate conditions, further demonstrating the utility of classifier-based adaptation in agriculture.

To cope with the high cost of labeling agricultural imagery, semi-supervised learning (SSL) and active learning (AL) have become increasingly prominent. Rajan et al. [52] proposed a Binary Hierarchical Classifier (BHC) that integrates SSL for continuous model updates in cross-year pest monitoring. Additionally, enhancements to the classic Domain Adaptation SVM (DASVM) have enabled improved generalization in cross-sensor crop classification with minimal labeled target samples [53].

Figure 7 illustrates the flowchart of a typical AL method for domain adaptation. Initially, a classifier is trained on the source domain and used to label the target domain. Samples with the highest prediction uncertainty are selected for manual labeling and added back to the training set, iteratively refining the classifier. AL is highly effective in precision agriculture due to its ability to reduce annotation demands. Deng et al. [54] developed an Active Multi-Kernel Domain Adaptation (AMKDA) method combining AL with multi-kernel learning, substantially reducing the need for labeled hyperspectral data. Kalita et al. [55] introduced a standard deviation (SD)-based AL strategy to identify the most informative samples, while Saboori et al. [56] proposed Active Multi-Kernel Fredholm Learning (AMKFL), which uses Fredholm regularization to guide annotation and improve classification.

To address morphological and scale variations in agricultural imagery, innovative classifiers have been introduced. Izquierdo-Verdiguier et al. [57] proposed the Virtual Support Vector (VSV) classifier, which incorporates rotation and scale invariance, achieving up to a 12% improvement in UAV-based farmland classification. Wang et al. [58] developed EasyTL, a non-parametric transfer method suitable for edge computing, enabling real-time crop status recognition with high adaptability in resource-limited agricultural environments.

### 3.4. Summary of Shallow DA Methods

Shallow Domain Adaptation (DA) methods primarily rely on traditional machine learning algorithms and handcrafted feature representations to mitigate distributional discrepancies between the source and target domains. These approaches can be broadly categorized into three types: instance weighting, feature transformation, and classifier-based adaptation. Instance-based methods reweight source domain samples based on their relevance to the target domain, thereby reducing marginal distribution shifts. Feature transformation techniques aim to project both domains into a shared, domain-invariant subspace to achieve feature-level alignment. Classifier-based adaptation methods focus on modifying classifier parameters to better generalize to target domain data.

The key advantages of shallow DA methods include their low computational complexity, ease of implementation, and reduced dependency on large-scale computational resources. These traits make shallow approaches particularly suitable for agricultural applications in resource-limited environments, such as edge computing systems or developing regions.

However, shallow methods exhibit notable limitations when applied to high-dimensional, structurally complex, and large-scale agricultural datasets. Due to their limited capacity for hierarchical feature extraction, they often struggle to model nonlinear relationships and contextual dependencies inherent in real-world agricultural scenarios. In cases involving substantial domain shifts—such as cross-regional crop mapping or multi-seasonal disease detection—shallow methods are generally inadequate for capturing deep semantic correlations, which compromises their generalization performance.

These limitations have catalyzed the adoption of deep learning-based domain adaptation techniques. The ability of deep models to learn rich, multi-level feature representations and capture complex domain-specific patterns has made them a powerful alternative to traditional methods, offering more robust and scalable solutions for cross-domain agricultural image analysis.

## 4. Deep Domain Adaptation (DA) Methods

With the rapid advancement of deep learning technologies, domain adaptation (DA) methods based on deep neural networks have demonstrated notable advantages in agricultural image analysis. These methods automatically extract domain-invariant features through end-to-end feature learning and distribution alignment, effectively mitigating domain shift problems caused by variations in sensors, environmental conditions, and crop growth stages. Depending on the availability of labeled data in the target domain, deep DA methods are typically classified into supervised, semi-supervised, and unsupervised approaches. This section provides a systematic review of their core principles and recent developments in agricultural applications.

### 4.1. Supervised Deep DA

Supervised deep DA methods assume access to a limited amount of labeled data in the target domain. These methods jointly optimize the feature extractor and classifier by minimizing a combination of source domain classification loss and cross-domain alignment loss. The primary idea is to construct a deep neural network that incorporates target domain label supervision into the domain alignment process. A typical supervised deep DA model consists of three modules: a feature extractor, a classifier, and a domain discrepancy measurement component. The joint loss function is formulated as:

$$L = L_{cls}(X_s, Y_s) + \lambda \cdot L_{align}(X_s, X_t) \quad (5)$$

Here,  $L_{cls}(X_s, Y_s)$  denotes the classification loss on the source domain,  $L_{align}(X_s, X_t)$  measures domain discrepancy (e.g., via MMD, adversarial loss, or covariance alignment), and  $\lambda$  is a trade-off parameter.

In agricultural scenarios, supervised deep DA is widely used for cross-sensor data fusion and multi-temporal crop monitoring. For instance, Takahashi et al. [35] proposed a category-aware adversarial learning framework that leverages source domain class labels to guide feature space alignment, thereby enhancing generalization on target agricultural datasets collected from heterogeneous imaging devices.

This approach comprises three main stages: image generation, transfer learning, and domain adaptation based on deep neural networks (DNNs). First, a Class Propagation Network (CPN) generates class maps from target images, simulating realistic agricultural image distributions. Second, transfer learning is performed on both real images ( $I$ ) and synthetic images ( $W$ ), producing two transfer models, TL-I and TL-W. Finally, deep networks implement domain adaptation using two modules: DA-W2I (synthetic-to-real adaptation) and DA-I2W (real-to-synthetic adaptation).

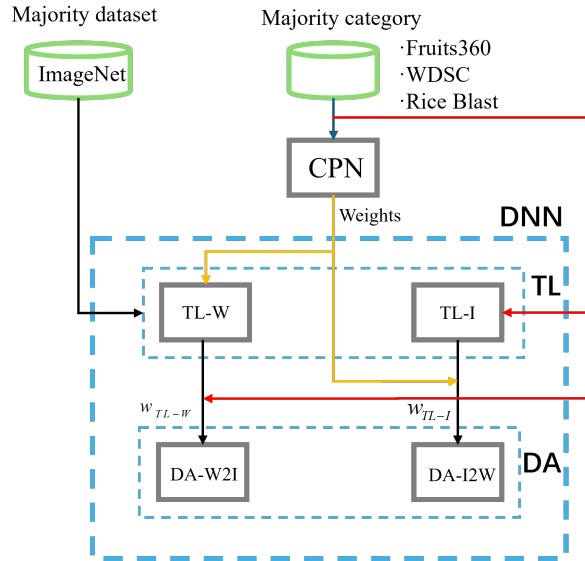


**Figure 8:** Structure of the method by Takahashi et al. [35].

As shown in Figure 8, the system architecture includes five components: CPN for image generation, TL-I and TL-W for transfer learning, and DA-W2I and DA-I2W for bi-directional domain adaptation [59]. These modules synergistically enhance generalization on the agricultural target domain, especially under limited label availability, leveraging both image-level and feature-level adaptation strategies. Similarly, Espejo-García et al. [60] proposed a method that integrates agricultural transfer learning with Generative Adversarial Networks (GANs) to synthesize annotated images, addressing the scarcity of labeled data in agricultural datasets.

Supervised convolutional neural networks (CNNs) have also shown strong performance in image segmentation tasks. In agricultural remote sensing, fully supervised CNNs have been applied to farmland boundary extraction. Lu et al. [61] introduced an attention mechanism to focus on critical spatial features and designed a feature fusion module for enhanced segmentation. However, low-resolution feature maps may cause blurred boundaries due to upsampling. To mitigate this, Li et al. [62] proposed a pixel-wise contextual modeling approach with post-processing to improve boundary clarity.

To further address scale variation issues, Shang et al. [63] presented a multi-scale object extraction framework with attention mechanisms, enabling adaptive segmentation of agricultural objects with diverse sizes. Zhang et al. [64] reformulated farmland extraction as an edge detection problem and developed a High-Resolution Boundary Refinement Network (HBRNet) to improve boundary precision.

Nevertheless, the application of supervised deep DA in real-world agriculture remains constrained by the high cost of acquiring labeled target domain samples. For instance, in the Cityscapes dataset [65], manual annotation of a single natural scene image requires approximately 1.5 hours. This limitation underscores the growing importance of semi-supervised and unsupervised DA paradigms, which are increasingly favored for their ability to leverage unlabeled data and reduce annotation overhead in practical agricultural deployments.

#### 4.2. Semi-supervised Deep Domain Adaptation (DA)

Semi-supervised Deep Domain Adaptation (DA) methods utilize fully labeled samples from the source domain along with a limited amount of labeled or pseudo-labeled data from the target domain. These approaches implement domain transfer through strategies such as self-training, co-training, and hybrid supervision. Their primary advantage lies in striking a balance between annotation cost and model performance, making them particularly valuable in agricultural scenarios characterized by scarce labeled target data.

Self-training and pseudo-label generation are core techniques in semi-supervised DA. Recent innovations have integrated diffusion models into this paradigm, showing promising results in agricultural applications. Ghanbari et al. [66] proposed a framework that combines diffusion models with meta-learning to perform wheat ear segmentation

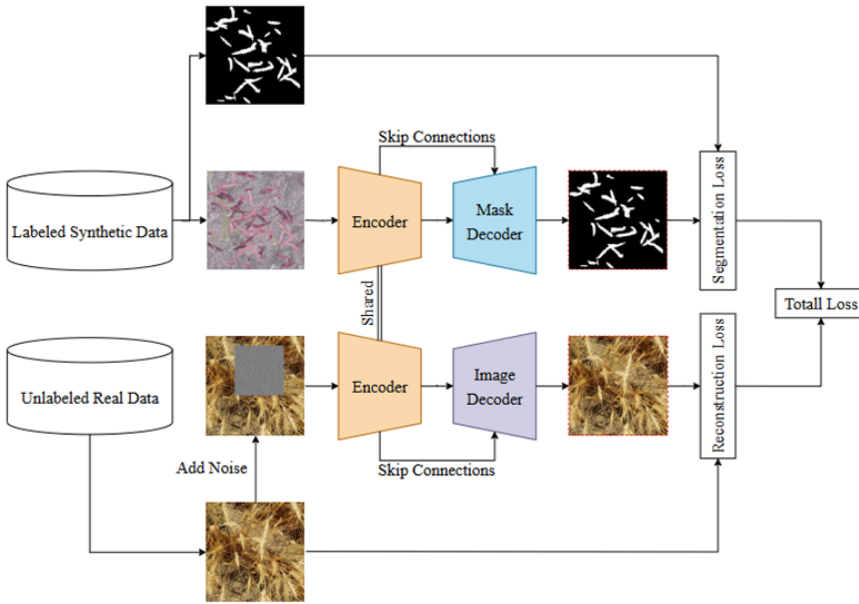


**Figure 9:** Schematic of the model architecture in Ghanbari’s method [66].

using only a few annotated samples. Specifically, the method requires just three manually labeled wheat images and unlabeled video frames to generate a large pseudo-labeled dataset through a probabilistic diffusion process.

The architecture incorporates a dual-branch encoder-decoder network designed to facilitate effective feature alignment and maintain semantic consistency between domains, as shown in Figure 9. The model achieved a Dice score of 63.5% on an external test set comprising farmland images from multiple countries, demonstrating strong generalization capabilities. This diffusion-based pseudo-labeling mechanism substantially improves the adaptability of deep DA in data-scarce agricultural environments, offering both scalability and practical relevance.

In this architecture, the encoder learns joint representations for both synthetic and real images, while the mask decoder generates segmentation masks. The image decoder reconstructs real images, encouraging the encoder to adapt to real domain features. Experimental results demonstrate Dice scores of 80.7% on internal test sets and 64.8% on external test sets from 18 plots across five countries. These results highlight the framework’s potential to support generalizable agricultural vision models and facilitate real-world deployment. By incorporating diffusion models, this approach effectively harnesses large-scale unlabeled datasets and has shown strong performance in image processing tasks [67, 68], underscoring its relevance in precision agriculture.

To address wheat disease detection, Najafian et al. [69] developed the WheatSeedBelt dataset and designed a pipeline combining pretrained models with semi-supervised fine-tuning, achieving high accuracy in Fusarium-damaged kernel (FDK) classification. Subsequently, they proposed a semi-self-supervised wheat head detection method [70], using a few annotated images and video sequences to generate pseudo-labeled datasets enhanced by domain adaptation techniques (mAP = 0.827).

Furthermore, they introduced a hybrid approach leveraging synthetic data and multi-domain adaptation for wheat head segmentation [71]. With only two labeled samples, their model achieved a Dice score of 0.89 on internal data and 0.91 after fine-tuning on diverse external data. This greatly enhances model generalization under label-scarce conditions, demonstrating practical viability for real-world deployment.

In vegetable detection, Yang et al. [72] proposed TDA-YOLO, a YOLOv5-based model adapted for tomato detection in densely planted fields under variable lighting. The model employs neural preset color style transfer to generate a pseudo dataset, narrowing the domain gap. Semi-supervised learning and knowledge distillation further enhance target domain adaptability, while the lightweight FasterNet backbone improves inference speed. Zhu et al. [73] introduced Semi-supervised Center-based Discriminative Adversarial Learning (SCDAL) for domain-adaptive aerial scene classification. Center-loss-guided adversarial learning strengthens domain discriminability. Teng et al. [74] proposed the Classifier-constrained Deep Adversarial Domain Adaptation (CDADA) method, which integrates the

Maximum Classifier Discrepancy (MCD) framework with deep convolutional neural networks (DCNNs) to enable semi-supervised cross-domain classification in remote sensing by adversarially aligning feature distributions.

In summary, semi-supervised domain adaptation effectively leverages limited labeled data to guide feature alignment, reduce annotation burdens, and improve model robustness across varied agricultural environments. These approaches provide practical solutions for multimodal data fusion and stage-aware crop monitoring—both essential components of precision agriculture.

### 4.3. Unsupervised Deep Domain Adaptation (DA)

Unsupervised Deep Domain Adaptation (Unsupervised Deep DA) fully leverages labeled source domain data and unlabeled target domain samples to achieve domain-invariant representation learning through feature space transformation or generative models [75, 76]. These approaches can be categorized into adversarial-based methods, discrepancy-based methods, and self-supervised learning, demonstrating significant value in annotation-scarce scenarios such as agricultural robotics and remote sensing mapping [77].

#### 4.3.1. Adversarial Training

Adversarial training, particularly via **Generative Adversarial Networks (GANs)**, is widely employed in Unsupervised Domain Adaptation (UDA), primarily for aligning the data distributions of the source and target domains. Two of the most influential adversarial training techniques are the **Domain-Adversarial Neural Network (DANN)** and the **Gradient Reversal Layer (GRL)**, both of which are conceptually derived from the GAN framework.

GANs, as a class of deep generative models [78], are typically applied in tasks involving image synthesis. Training a GAN requires a dataset representative of the desired target domain, such as CelebA for facial images [79], MNIST for handwritten digits [80], LSUN for bedroom scenes [81], or general object categories like CIFAR-10 [82] and ImageNet [83]. Once trained, the generative model can synthesize images that closely resemble real samples from the training set.

As illustrated in Figure 10, a GAN consists of two neural networks in competition [84]:

- The **generator** takes a noise vector as input (typically sampled from a uniform or Gaussian distribution) and attempts to generate synthetic samples that are indistinguishable from real data.
- The **discriminator** receives either real samples from the dataset or fake samples from the generator and aims to distinguish between them.

During training, these two networks play a *minimax game*, in which the generator seeks to fool the discriminator, while the discriminator learns to avoid being deceived. According to Goodfellow et al. [78], this game is defined by the following value function:

$$\min_G \max_D V(D, G) = \mathbb{E}_{x \sim P_{\text{data}}(x)} [\log D(x)] + \mathbb{E}_{z \sim P_z(z)} [\log(1 - D(G(z)))] \quad (6)$$

Here,  $x \sim P_{\text{data}}(x)$  denotes a real sample from the data distribution,  $z \sim P_z(z)$  is a noise vector sampled from a prior distribution,  $D(x; \theta_d)$  is the discriminator's probability output for classifying  $x$  as real, and  $G(z; \theta_g)$  is the generator's output given noise  $z$ .

The objective for the discriminator  $D$  is to *maximize* the probability of correctly classifying real and fake samples, while the generator  $G$  aims to *minimize* the probability that its fake outputs are correctly identified. That is, when  $D(G(z)) = 0$ , the discriminator perfectly identifies fake data, and when  $D(G(z)) = 1$ , the generator has successfully fooled the discriminator.

This adversarial process allows the generator to continuously improve its outputs, ultimately leading to the generation of highly realistic synthetic samples. GANs have proven especially valuable in domain adaptation tasks involving significant visual discrepancies between domains, such as style transfer between different sensors in agricultural remote sensing.

In adversarial training, **Generative Adversarial Networks (GANs)**—such as CycleGAN—and **Discriminative Adversarial Networks (DANN)** serve distinct purposes and exhibit different application scenarios. GANs are primarily designed to synthesize data samples, making them especially suitable for tasks such as image style transfer and image generation. In contrast, discriminative adversarial networks focus on aligning feature distributions between domains and are commonly applied in feature representation learning and domain adaptation tasks.

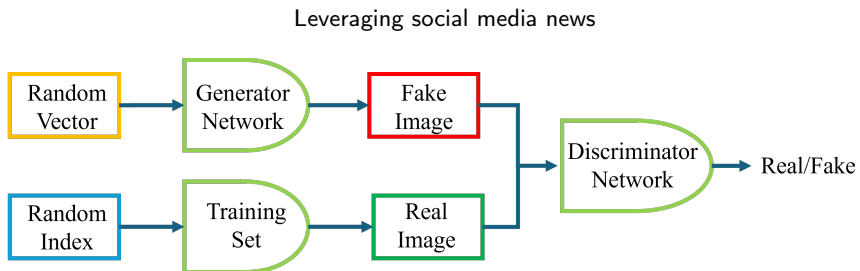


**Figure 10:** Principle diagram of GAN adversarial training. The generator attempts to produce realistic samples, while the discriminator learns to distinguish real from synthetic data.

A typical GAN consists of two components: a generator and a discriminator. The generator is trained to produce target domain samples based on the distribution of source domain data, while the discriminator attempts to distinguish real samples from generated ones. In the agricultural domain, GANs have been extensively used for cross-sensor image style transfer. For instance, CycleGAN has been applied to transform the visual style of source domain remote sensing imagery to resemble that of the target sensor, thus mitigating domain shifts [85]. Zhang [86] proposed an unsupervised adversarial domain adaptation method for agricultural land extraction, as illustrated in Figure 11, introducing a multi-scale feature fusion (MSFF) module to adapt across datasets with varying spatial resolutions. This design enhances the model’s robustness in learning domain-invariant features.

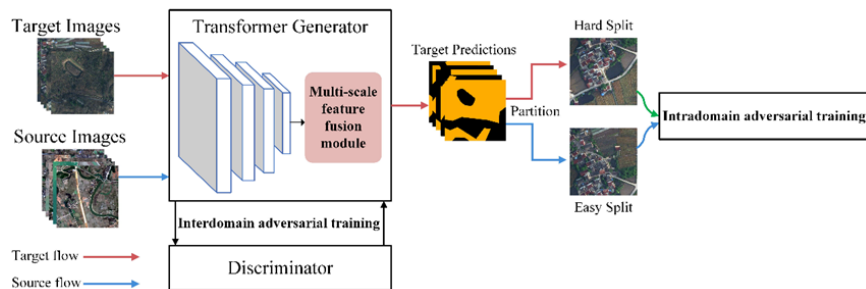


**Figure 11:** Multi-Scale Cross-Domain Adversarial Training and Feature Fusion Framework by Zhang [86].

Ji et al. [87] introduced an end-to-end GAN-based DA framework for land cover classification using multi-source imagery. In this approach, source images are translated into the target style via adversarial learning, and semantic segmentation is performed using a fully convolutional network (FCN). Similarly, Tasar et al. [88] proposed a standard GAN-based DA pipeline for semantic segmentation of very high-resolution (VHR) satellite images and extended it to a multi-source, multi-target, and lifelong learning setting. Wittich et al. [89] designed a Color Map GAN for consistent appearance adaptation in aerial image classification. Liu et al. [90] developed a GAN-based feature extractor for agricultural scene classification that enhances cross-domain classification accuracy by aligning source and target distributions. While GANs perform exceptionally well in unpaired style transfer tasks, their major drawbacks include susceptibility to mode collapse and high computational cost during training.

On the other hand, **Discriminative Adversarial Networks**, such as DANN, as illustrated in Figure 12, incorporate a domain classifier that distinguishes between source and target domain features. During training, a gradient reversal layer enables backpropagation to align feature distributions implicitly, thus improving the generalization capacity of the learned model in the target domain. In agriculture, DANN has been widely adopted for domain-invariant feature extraction and alignment.

For example, Yan et al. [91] proposed a Tri-Adversarial Domain Adaptation (TriADA) framework for pixel-level classification in VHR remote sensing images, which incorporates a domain similarity discriminator to learn transferable classifiers. Wang et al. [92] proposed an Adversarial Domain Adaptation (ADDA) approach for cross-device calibration in hyperspectral imaging systems, aligning spectral distributions across devices (e.g., HySpex and Headwall). Their method achieved a 21.5% reduction in RMSE for predicting relative water content (RWC) in maize, highlighting the method's effectiveness in cross-platform model transfer.

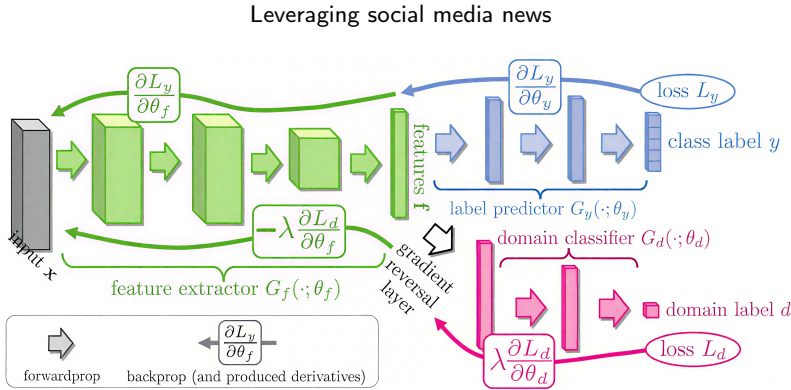


**Figure 12:** Basic Network Architecture of DANN for Cross-Domain Feature Alignment.

Additional applications of DANN in agricultural image analysis include Bejiga et al. [93], who applied a DANN-based model for large-scale land cover classification using multispectral data. Rahhal et al. [94] designed a multi-source DA strategy using a min-max entropy optimization technique. Elshamli et al. [95] combined denoising autoencoders (DAEs) with DANN to handle DA in multi-temporal and multi-spatial imagery. Mauro et al. [96] integrated self-attention mechanisms into adversarial networks to address domain variance in multi-temporal land cover classification. Mateo et al. [97] proposed a cross-sensor adversarial DA method for cloud detection using Landsat-8 and Proba-V imagery. Ma et al. [98] introduced an Adaptive DANN (ADANN) framework that aligns meteorological features and vegetation indices across U.S. agricultural zones, achieving a 34.1% reduction in yield prediction RMSE. Discriminative adversarial networks offer the advantage of low annotation dependency while significantly enhancing cross-domain generalization. However, they are sensitive to feature extractor quality and may exhibit convergence instability under large domain gaps.

Adversarial DA strategies, including hybrid GAN-DANN frameworks, are being widely used in remote sensing tasks such as scene classification [85], crop classification [99], road extraction [84], and cloud detection [100]. Nonetheless, the use of fixed distance metrics (e.g., MMD) may not suffice for diverse agricultural imagery datasets. Recent advances further refined adversarial DA. Hoffman et al. [101] first integrated adversarial training into pixel-level domain adaptation. Tsai et al. [102] proposed AdaptSegNet to reduce domain shifts at the segmentation output level. Vu et al. [103] introduced ADVENT, which applies entropy-based adversarial loss to segmentation outputs. Li et al. [104] proposed a bi-directional learning (BDL) approach to enhance bidirectional feature alignment. Zhang et al. [105] designed DFEENet, a domain feature enhancement network that models both channel and spatial dependencies to improve discriminability. Zheng et al. [106] presented TSAN, a two-stage adaptive network for multi-target remote sensing scene classification. Rahhal et al. [94] again applied multi-source adversarial adaptation using entropy-based alignment. Makkar et al. [107] used adversarial learning to extract target-discriminative geospatial features. Finally, Saito et al. [108] proposed an open-set adversarial DA framework that explicitly separates known and unknown target classes. During training, the feature generator either aligns the sample with known source categories or rejects it as an unknown sample, effectively supporting open-set classification in domain shift scenarios.

#### 4.3.2. Discrepancy-Based Alignment

Discrepancy-based deep domain adaptation (DA) methods aim to reduce the divergence between marginal and/or conditional distributions of the source and target domains by incorporating distribution alignment metrics—such as Maximum Mean Discrepancy (MMD)—into deep neural network architectures [109]. These strategies typically employ additional alignment layers to encourage the learning of domain-invariant, task-relevant representations, as illustrated in Figure 13.

Long et al. [110] pioneered the Deep Adaptation Network (DAN), which extends convolutional neural networks for domain adaptation by aligning the distributions of learned features across domains. Baktashmotagh et al. [111] proposed a domain-invariant projection method using MMD, while Shen et al. [112] introduced the Wasserstein Distance Guided Representation Learning (WDGRL) framework. Sun et al. [113] extended the CORAL framework with Deep CORAL, aligning activation correlations in deep layers through nonlinear transformations.

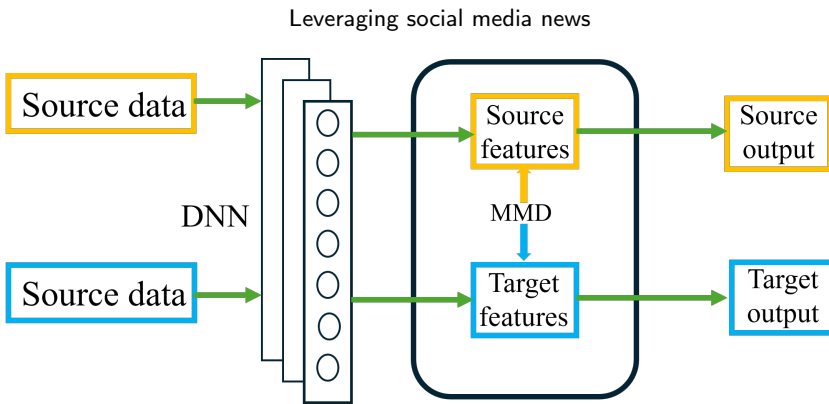


**Figure 13:** Flowchart of discrepancy-based deep DA methods.

In agriculture, Ferreira [114] proposed an unsupervised domain adaptation framework based on vision Transformers (UDA-SegFormer) to enhance crop row and gap detection across farms. By aligning domain-specific features and simplifying pseudo-labels, the model achieved superior generalization in challenging environments (e.g., shadows, curved rows), outperforming traditional CNN-based networks such as PSPNet and DeepLabV3+. This work represents the first integration of Transformers with UDA in agricultural contexts, enabling label-efficient and robust crop monitoring.

Guo et al. [115] propose masked image consistency and multi-granularity alignment to enhance domain adaptation for plant disease detection. Their method reduces domain shift between source and target data, improving cross-domain robustness. This approach achieves state-of-the-art performance in agricultural disease recognition. Gao et al. [116] develop a cross-domain transfer learning framework for weed segmentation using both ground and UAV images. Their model bridges domain gaps between aerial and ground-level perspectives in precision farming. The solution enables accurate weed mapping for targeted agricultural management. Fu et al. [117] introduce a multi-domain data augmentation strategy combined with isolated test-time adaptation for crop disease detection. This dual approach enhances model generalization to unseen field conditions without source data access. Their method significantly improves robustness against domain shifts.

Takahashi et al. [35] enhanced agricultural image recognition via category-wise feature space alignment. Building on DAN, Long et al. [118] proposed the Multi-Representation Adaptation Network (MRAN) [119] and the Deep Sub-domain Adaptation Network (DSAN) [120], which utilize sub-domain partitioning and multi-representation learning to better address inter-domain variability.

Real-world high-resolution satellite (HRS) imagery often varies across regions in terms of scale, resolution, and spectral characteristics [121]. To address this heterogeneity, Zhu et al. [122] proposed the Weak Pseudo-supervised Decorrelation Sub-domain Adaptation (WPS-DSA) network for land use classification, which effectively handles both spatial and temporal feature distribution shifts.

In the field of cotton boll status recognition, Li [123] introduced NCADA, an unsupervised DA method based on Neighborhood Component Analysis, along with the first benchmark dataset for in-field cotton boll imagery, as shown in Figure 14. NCADA outperformed traditional classification methods and achieved competitive accuracy under real-world distribution shifts, paving the way for automated phenotyping in precision agriculture.

For hyperspectral image (HSI) domain adaptation, Garea et al. [124] introduced TCANet, which integrates Transfer Component Analysis (TCA) into a deep network. Ian et al. [78] developed DDA-Net to facilitate unsupervised knowledge transfer across HSI datasets. Li et al. [125] proposed a two-stage deep domain adaptation (TDDA) framework: Stage I minimizes MMD-based domain shifts via deep embedding; Stage II employs a spatial-spectral twin network to extract discriminative features. Zhang et al. [126] presented TST-Net, which combines graph convolutional networks (GCNs) and convolutional layers to encode both topological and semantic information for cross-scene classification. Wang et al. [127] proposed a GNN-based DA model that jointly aligns domain and class distributions through CORAL integration. Liang et al. [128] proposed AMF-FSL, an attention-driven few-shot learning framework for HSI classification that incorporates target-class alignment, domain attention, and multi-source fusion modules.

In plant pathology, Yan et al. [129] designed a hybrid sub-domain alignment strategy for cross-species plant disease severity recognition. Fuentes et al. [130] developed a domain-adaptive classification model for tomato diseases



**Figure 14:** Example images from the In-field Cotton Boll (IFCB) dataset.

that accounts for environmental variability. However, these approaches often fail to address the full complexity of cross-species disease diagnosis. To this end, Wu [131] proposed MSUN, a multi-representation sub-domain alignment network with uncertainty regularization. MSUN effectively addresses intra-domain ambiguity, inter-class overlap, and inter-domain heterogeneity—key challenges in plant disease recognition across species.

Othman et al. [132] introduced a DA network for cross-scene classification, utilizing a two-stage training strategy combining pretraining and fine-tuning. Their approach ensures accurate classification of source-domain samples while aligning feature distributions between domains and preserving the geometric structure of target-domain data. Similarly, Lu et al. [133] proposed the Multi-Source Compensation Network (MSCN), which incorporates both cross-domain alignment modules and classifier compensation mechanisms to jointly reduce domain shift and align class semantics across multiple source domains. Zhu et al. [134] developed the Attention-based Multi-Scale Residual Adaptation Network (AMRAN), which includes a residual adaptation module for marginal distribution alignment, an attention module for feature enhancement, and a multi-scale adaptation module for conditional distribution alignment. In the SAR image domain, Geng et al. [135] proposed the Deep Joint Distribution Adaptation Network (DJDAN), which simultaneously aligns marginal and conditional distributions to facilitate transfer learning in SAR image classification.

Recently, self-supervised learning (SSL) has emerged as a powerful paradigm in the absence of labeled data, offering strong capabilities in feature representation learning [136]. Zhao et al. [137] proposed the Contrastive Learning and Domain Adaptation Layer (CLA) framework for leaf disease recognition, which innovatively combines self-supervised pretraining with fine-tuned domain adaptation. This two-stage approach is particularly effective for agricultural scenarios with large-scale unlabeled datasets.

In the self-supervised pretraining stage, CLA employs contrastive learning to train an encoder on a large pool of unlabeled, domain-confounded images. The objective is to maximize the similarity between augmented views of the same image (positive pairs) while minimizing similarity between different images (negative pairs), similar to the contrastive loss used in SimCLR.

In the second stage, CLA fine-tunes the learned representations with limited labeled data using a Domain Adaptation Layer (DAL), which jointly optimizes supervised loss and domain alignment loss. The total loss function is defined as:

$$L_{\text{DAL}} = L_{\text{supervised}} + \lambda \cdot L_{\text{MMD}} \quad (7)$$

Where:  $L_{\text{supervised}}$  is the classification loss on labeled data,  $L_{\text{MMD}}$  is the Maximum Mean Discrepancy-based alignment loss, and  $\lambda$  is a trade-off hyperparameter.

Experimental results show that CLA significantly outperforms baseline and comparison models in both domain alignment and final classification accuracy, achieving a peak accuracy of 90.52%. Further ablation and sensitivity analyses reveal key contributing factors, offering deeper insights into its mechanism.

The CLA framework exemplifies the effective combination of self-supervised contrastive learning and domain adaptation to enhance generalization performance in leaf disease recognition under low-label regimes. Its ability to leverage unlabeled data while mitigating domain shift makes it a scalable and label-efficient solution for intelligent plant health monitoring systems.

#### 4.4. Summary of Deep Domain Adaptation (DA) Methods

With the rapid advancement of deep learning technologies, deep domain adaptation (DA) methods have demonstrated significant advantages in agricultural image analysis. These approaches, based on deep neural networks (DNNs) and adversarial training, are capable of automatically learning domain-invariant feature representations, effectively addressing the challenges posed by domain shift. Deep DA methods are typically categorized into supervised, semi-supervised, and unsupervised frameworks.

In supervised deep DA methods, the source-domain classification loss and cross-domain alignment loss are jointly optimized to align the feature distributions between source and target domains. This enhances the model's generalization capability in the target domain. Semi-supervised deep DA methods utilize fully labeled source-domain data along with a small portion of labeled target-domain data. By balancing annotation costs and model performance, these methods are particularly suitable for agricultural scenarios where labeled target data is scarce.

Unsupervised deep DA methods rely exclusively on labeled data from the source domain and unlabeled data from the target domain. Domain adaptation is achieved through feature alignment strategies (e.g., adversarial learning, distribution matching) or generative models (e.g., GAN-based feature synthesis), making them widely applicable in real-world agricultural tasks.

The key advantage of deep DA methods lies in their ability to process high-dimensional, complex agricultural data and extract domain-invariant representations via end-to-end training. This enables effective mitigation of domain discrepancies caused by sensor variability, environmental heterogeneity, and crop phenological stages. However, these methods also face several challenges, such as high computational demands, prolonged training times, and limited interpretability. These drawbacks may constrain their deployment in resource-limited environments or scenarios requiring real-time performance.

Despite these limitations, ongoing advancements in model efficiency, interpretability, and hardware acceleration continue to expand the potential of deep DA methods. They are expected to play an increasingly critical role in the development of precision agriculture and intelligent farming systems.

### 5. Experimental Results: Evaluation, Comparison, and Analysis

To effectively demonstrate the superiority of deep domain adaptation (DA) methods in agricultural applications, this section presents experimental results on three core tasks: plant disease detection, crop yield prediction, and agricultural land extraction from remote sensing imagery. Both quantitative metrics and visual results are used to assess model performance.

#### 5.1. Datasets Overview

The experiments conducted in this study utilize several prominent agricultural image datasets to evaluate domain adaptation techniques effectively. Specifically, the remote sensing datasets include:

- **DeepGlobe:** Primarily employed for urban and rural land-cover classification and segmentation. Download via Dataset Ninja or official DeepGlobe 2018 Challenge website.
- **GID:** Used extensively for high-resolution land-use and land-cover mapping. Official site: <https://captain-whu.github.io/GID/>, with OneDrive/Baidu download links.
- **LoveDA:** Designed for detailed semantic segmentation tasks including agricultural and geographic information extraction. GitHub repository at <https://github.com/Junjue-Wang/LoveDA>, with dataset hosted on Zenodo.

For crop disease detection and classification tasks, the datasets employed are:

- **PlantVillage:** Widely used for benchmarking plant disease classification methods under controlled laboratory conditions. Available on Kaggle: <https://www.kaggle.com/datasets/emmarex/plantdisease> and GitHub.
- **PlantDoc:** Targeted toward real-world plant disease diagnosis under diverse environmental conditions. GitHub repository (PlantDoc-Dataset) and listed on Papers With Code.

**Table 2**  
Summary of datasets used in the experiments

Dataset	Resolution	Sensor	Image Size	Training Set	Test Set
DeepGlobe	0.5 m/pixel	WorldView-2	2448 × 2448	30,470	N/A
GID	4 m/pixel	GF-2	6800 × 7200	73,490	734
LovedA	0.3 m/pixel	Spaceborne	1024 × 1024	15,829	324
PlantVillage	256 × 256	RGB	Fixed size	50,000	5,000
PlantDoc	Variable	RGB	Variable	2,000	500
Plant-Pathology	2048 × 1365	RGB	Fixed size	2,921	730
Corn-Leaf-Diseases	256 × 256	RGB	Fixed size	2,500	500
Tomato-Leaf-Diseases	256 × 256	RGB	Fixed size	4,000	1,000
NASS	N/A	Tabular Data	Multi-year (regionwise)	N/A	N/A

- **Plant-Pathology:** Employed for identification and severity assessment of foliar diseases. Provided through the Kaggle FGVC8 competition.
- **Corn-Leaf-Diseases:** Specifically developed for maize disease detection. Available on Kaggle as “Corn or Maize Leaf Disease Dataset”.
- **Tomato-Leaf-Diseases:** Focused on tomato leaf disease monitoring. Downloadable from Kaggle or Mendeley Data.

Additionally, the following dataset provides tabular agricultural data:

- **NASS:** Widely applied in crop yield prediction, agricultural policy analysis, and cross-domain productivity modeling. Available from the official USDA NASS portal: <https://www.nass.usda.gov>.

A summary of these datasets—including spatial resolution, sensor type, image dimensions, data partitioning, and their respective application scenarios—is presented in Table 2. Collectively, these datasets represent a comprehensive range of agricultural scenarios, sensor modalities, and domain challenges, thereby serving as robust benchmarks for evaluating domain adaptation approaches in agricultural image analysis.

## 5.2. Evaluation Metrics

We adopt a diverse set of evaluation metrics to comprehensively assess the performance of classification, regression, and segmentation models in agricultural image analysis. The definitions and corresponding formulas are provided below.

### Average Accuracy (AA)

$$\text{AA} = \frac{1}{C} \sum_{i=1}^C \frac{N_{ii}}{\sum_{j=1}^C N_{ij}} \quad (8)$$

Where:  $C$  is the number of classes, and  $N_{ij}$  denotes the number of samples with true label  $i$  predicted as class  $j$ . This metric assigns equal weight to each class, mitigating the effects of class imbalance.

### Root Mean Squared Error (RMSE)

$$\text{RMSE} = \sqrt{\frac{1}{n} \sum_{i=1}^n (y_i - \hat{y}_i)^2} \quad (9)$$

Where:  $y_i$  is the ground truth value, and  $\hat{y}_i$  is the predicted value. RMSE expresses the prediction error in the same units as the target variable and is widely used in regression tasks.

*Coefficient of Determination ( $R^2$ )*

$$R^2 = 1 - \frac{\sum_{i=1}^n (y_i - \hat{y}_i)^2}{\sum_{i=1}^n (y_i - \bar{y})^2} \quad (10)$$

Where:  $\bar{y}$  is the mean of the ground truth values. The  $R^2$  score quantifies the proportion of variance in the dependent variable that is predictable from the independent variables.

*Intersection over Union (IoU)*

$$\text{IoU} = \frac{|P \cap G|}{|P \cup G|} \quad (11)$$

Where:  $P$  is the predicted region and  $G$  is the ground truth region. IoU is a standard metric for evaluating semantic segmentation performance.

*Completeness (COM)*

$$\text{COM} = \frac{\text{TP}}{\text{TP} + \text{FN}} \quad (12)$$

COM measures the proportion of actual agricultural land pixels that were correctly identified by the model.

*Correctness (COR)*

$$\text{COR} = \frac{\text{TP}}{\text{TP} + \text{FP}} \quad (13)$$

COR indicates the proportion of predicted agricultural land pixels that are truly correct.

*Segmentation F1 Score*

$$\text{F1}_{\text{seg}} = \frac{2 \cdot \text{COM} \cdot \text{COR}}{\text{COM} + \text{COR}} \quad (14)$$

This segmentation-specific F1 score harmonizes completeness and correctness to evaluate overall segmentation quality.

### 5.3. Plant Disease Detection Experiments

This section presents the classification, detection, and prediction capabilities of deep domain adaptation (DA) methods in agricultural scenarios. We evaluate plant disease detection, crop yield prediction, and remote sensing-based agricultural land extraction. Since the methods are trained and tested on different datasets, we unify the evaluation by selecting common benchmark datasets. The best-performing results are highlighted in **bold** to facilitate comparison.

To evaluate domain adaptation for plant disease detection, we conducted four sets of experiments using five benchmark datasets: PlantVillage (PVD) [138], PlantDoc [139], Plant-Pathology [140], Corn-Leaf-Diseases, and Tomato-Leaf-Diseases, as shown in Figure 15. Among them, PlantVillage (PVD) was consistently used as the source domain due to its controlled acquisition environment and clean backgrounds, which facilitate robust model training.

Table 3 summarizes the results of eight models—Baseline, DAAN, D-CORAL, DAN, DANN, MRAN, DSAN, and MSUN—on four transfer tasks: C-PD, PVD-PP, PVD-CLD, and PVD-TLD. Compared to the multi-crop mixed transfer scenario in C-PD, single-crop domain adaptation tasks (e.g., PVD-CLD and PVD-TLD) generally yield better performance due to more consistent intra-class boundaries. MSUN consistently achieves top accuracy across all settings, owing to its multi-representation learning and subdomain alignment mechanisms, which address high inter-class similarity and intra-class variability.

In the plant disease transfer detection task, MSUN demonstrates significant advantages across diverse experimental configurations. Whether in multi-crop mixed transfer (C-PD) or single-crop transfer (PVD-PP, PVD-CLD, PVD-TLD), MSUN consistently achieves superior average accuracy compared to state-of-the-art domain adaptation methods.

Specifically, in the C-PD task, MSUN achieves an average accuracy of 56.06%, outperforming the baseline by over 25 percentage points. It also surpasses advanced models such as DSAN and MRAN, showcasing strong adaptability to substantial domain shifts and complex inter-class relationships.

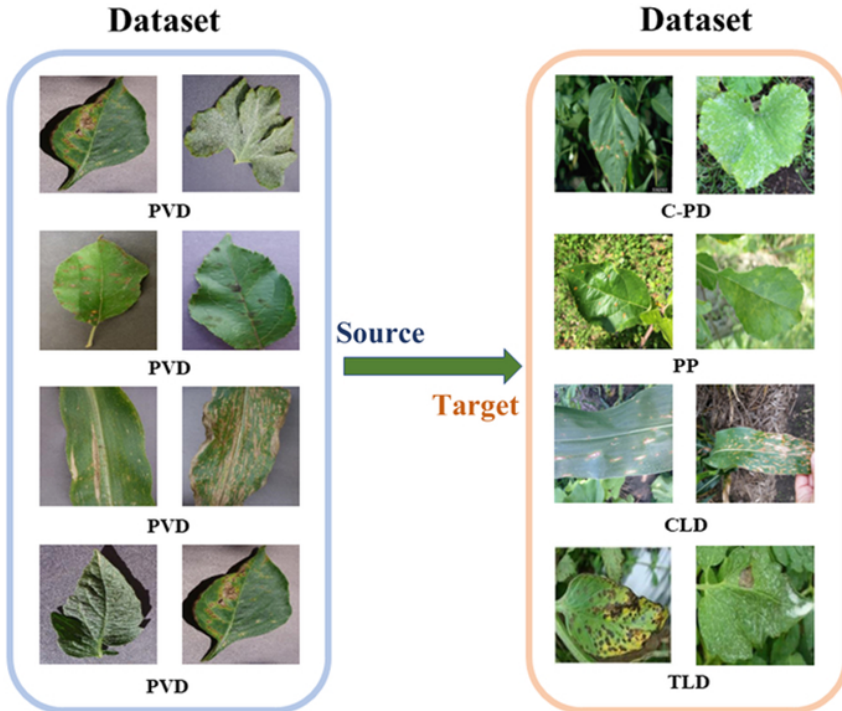


**Figure 15:** Domain adaptation setups for four experiments. Left: source domain dataset (PWD); Right: respective target domain datasets.

In the PVD-PP experiment, MSUN attains the highest accuracy across all three disease categories, reaching an average of 72.31%. It significantly outperforms MRAN (67.45%) and DANN (50.04%), highlighting its enhanced transferability in single-crop scenarios.

Under the PVD-CLD setting, MSUN achieves an outstanding average accuracy of 96.78%, particularly excelling in the “Blight” (93.81%) and “Healthy” (84.77%) classes. This underscores its strong capability in extracting discriminative features and reducing inter-class confusion.

The PVD-TLD task, characterized by fine-grained classes and severe data imbalance, poses greater challenges. While most methods show limited effectiveness, MSUN still achieves an average accuracy of 50.58%. Notably, it attains 80.79% accuracy in the low-sample “Septoria spot” category, indicating superior generalization to minority classes and robustness against sample imbalance.

Overall, MSUN exhibits consistent and leading performance across plant disease transfer tasks, validating the effectiveness of its multi-representation learning and subdomain alignment strategies. Compared to traditional domain adaptation approaches, MSUN not only enhances classification accuracy but also improves robustness and generalization under conditions of class imbalance, multi-disease complexity, and cross-crop variability.

#### 5.4. Crop Yield Prediction Experiments

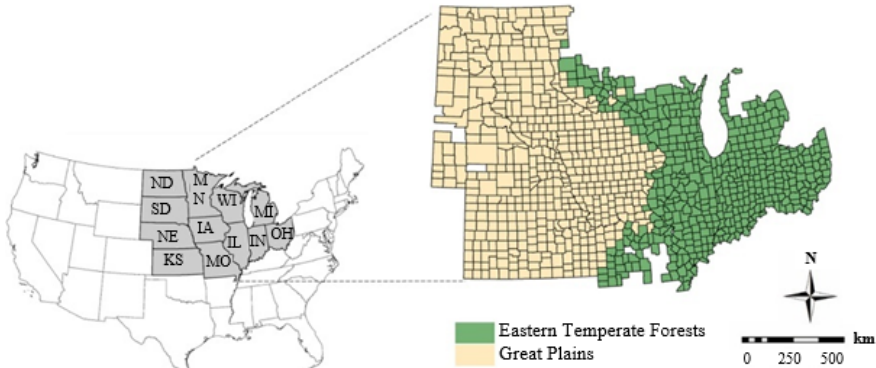
For crop yield prediction, we selected the U.S. Corn Belt as the study region—the world’s largest corn-producing area with abundant historical yield data. Model training incorporated three types of data: remote sensing products, meteorological observations, and crop yield records. All data were sourced from the USDA National Agricultural Statistics Service (NASS, 2020), as shown in Figure 16. The experiment included both local (intra-region) and cross-domain (inter-region) prediction tasks. We compared four models: Random Forest (RF), Deep Neural Network (DNN), Domain-Adversarial Neural Network (DANN), and an improved variant (ADANN).

Table 4 summarizes the prediction results across different years and transfer settings. In local experiments (e.g., GP→GP or ETF→ETF), DNN and ADANN generally outperform RF and DANN. In cross-domain settings (e.g., GP→ETF or ETF→GP), ADANN consistently achieves higher  $R^2$  scores and lower RMSE values, demonstrating its effectiveness in domain-invariant yield prediction.

**Table 3**

Accuracy (%) results across four experimental setups: C-PD, PVD-PP, PVD-CLD, and PVD-TLD.

Task	Class / Crop	Baseline	DAAN	D-CORAL	DAN	DANN	MRAN	DSAN	MSUN
C-PD	Apple	67.38	68.64	69.06	70.29	69.63	68.98	65.51	<b>71.45</b>
	Corn	50.07	48.81	49.11	52.15	48.11	49.87	51.39	<b>56.46</b>
	Grape	71.36	63.93	79.79	78.24	83.41	82.38	79.79	<b>85.49</b>
	Pepper bell	84.19	87.79	86.75	90.91	90.90	92.46	90.91	<b>93.49</b>
	Potato	50.34	63.66	66.06	64.72	62.33	57.82	64.19	<b>67.42</b>
	Tomato	30.17	39.82	43.32	46.23	49.51	49.34	45.75	<b>48.67</b>
	<b>Average</b>	30.78	33.08	33.37	33.79	39.71	39.84	42.87	<b>56.06</b>
PVD-PP	Gray spot	79.54	66.16	77.56	<b>89.02</b>	85.12	81.28	83.96	87.32
	Rust	24.10	55.81	33.42	34.99	30.26	52.57	35.42	<b>57.71</b>
	Healthy	11.02	36.64	48.05	11.84	28.71	70.87	51.24	<b>73.86</b>
	<b>Average</b>	39.27	53.75	52.41	48.89	50.04	67.45	56.41	<b>72.31</b>
PVD-CLD	Gray spot	61.49	78.57	79.44	68.29	76.66	79.22	<b>81.71</b>	80.09
	Blight	86.75	92.27	91.88	91.50	91.73	92.05	91.58	<b>93.81</b>
	Healthy	79.05	84.29	82.64	81.33	82.64	83.61	83.42	<b>84.77</b>
	Rust	99.18	<b>100.0</b>						
PVD-TLD	<b>Average</b>	75.96	90.35	89.90	87.89	89.47	91.06	90.69	<b>96.78</b>
	Bacterial spot	5.34	10.23	12.50	12.22	8.24	18.47	10.51	<b>29.27</b>
	Healthy	70.61	83.75	85.81	83.41	<b>86.92</b>	75.92	92.03	78.67
	Late blight	79.05	3.97	1.64	0.93	3.50	2.11	1.64	<b>3.28</b>
	Mold leaf	25.03	33.15	<b>37.43</b>	38.18	38.73	33.15	29.61	32.77
	Septoria spot	6.36	5.16	18.73	67.11	4.13	78.64	0.29	<b>80.79</b>
<b>Average</b>	21.46	30.96	32.31	42.80	28.71	44.86	27.57	<b>50.58</b>	

**Figure 16:** Corn planting counties in two ecosystem regions—Eastern Temperate Forest (ETF) and Great Plains (GP)—used in cross-domain prediction experiments. Image adapted from Ma et al. [41].

The results reveal that in local prediction experiments, both DNN and RF exhibit relatively stable performance, with DNN particularly excelling in the ETF→ETF setting. For instance, in 2019, DNN achieved an  $R^2$  of 0.71—the highest among all models that year—demonstrating strong capability in modeling same-domain data with structured and abundant samples.

In contrast, traditional models perform poorly in cross-domain scenarios (GP→ETF and ETF→GP). For example, in 2019, RF achieved an  $R^2$  of only 0.19 in the ETF→GP task, compared to 0.74 in the local GP→GP setting. This highlights the model's limited generalization under domain shift. DNN faced similar challenges, exhibiting substantial prediction variance and instability under domain transfer conditions.

Incorporating adversarial training significantly improves model robustness and generalization in cross-domain prediction. Both DANN and ADANN outperform RF and DNN in cross-domain tasks, with ADANN consistently

**Table 4**

Comparison of model performance in crop yield prediction across different years and transfer settings.

Year	Transfer Setting	Metric	RF	DNN	DANN	ADANN
2016	GP→GP	$R^2$	0.75	0.81	0.64	<b>0.85</b>
		RMSE	1.39	1.18	1.65	<b>1.05</b>
	ETF→ETF	$R^2$	0.51	0.55	0.47	<b>0.62</b>
		RMSE	1.13	1.01	1.18	<b>0.92</b>
	GP→ETF	$R^2$	0.54	0.43	0.44	<b>0.67</b>
		RMSE	1.02	1.22	1.21	<b>0.86</b>
	ETF→GP	$R^2$	0.48	0.55	0.68	<b>0.76</b>
		RMSE	1.98	1.82	1.54	<b>1.35</b>
2017	GP→GP	$R^2$	0.73	0.75	0.74	<b>0.77</b>
		RMSE	1.34	1.26	1.30	<b>1.24</b>
	ETF→ETF	$R^2$	0.61	0.75	0.64	<b>0.78</b>
		RMSE	1.23	0.97	1.17	<b>0.91</b>
	GP→ETF	$R^2$	0.58	0.52	0.35	<b>0.73</b>
		RMSE	1.26	1.36	1.58	<b>1.03</b>
	ETF→GP	$R^2$	0.52	0.64	0.68	<b>0.77</b>
		RMSE	1.78	1.54	1.45	<b>1.23</b>
2018	GP→GP	$R^2$	0.76	0.79	0.81	<b>0.84</b>
		RMSE	1.11	1.05	1.00	<b>0.91</b>
	ETF→ETF	$R^2$	0.54	0.56	0.51	<b>0.65</b>
		RMSE	0.97	0.95	1.00	<b>0.84</b>
	GP→ETF	$R^2$	0.49	0.30	0.33	<b>0.57</b>
		RMSE	1.01	1.20	1.17	<b>0.97</b>
	ETF→GP	$R^2$	0.53	0.49	0.75	<b>0.78</b>
		RMSE	1.57	1.63	1.14	<b>1.07</b>
2019	GP→GP	$R^2$	0.74	0.73	0.53	<b>0.76</b>
		RMSE	1.14	1.15	1.53	<b>1.08</b>
	ETF→ETF	$R^2$	0.63	0.71	0.64	<b>0.66</b>
		RMSE	1.09	0.96	1.08	<b>1.05</b>
	GP→ETF	$R^2$	0.52	0.56	0.62	<b>0.68</b>
		RMSE	1.25	1.19	1.11	<b>1.02</b>
	ETF→GP	$R^2$	0.19	0.34	0.56	<b>0.73</b>
		RMSE	2.00	1.80	1.47	<b>1.15</b>

delivering superior and more stable performance. For instance, in the 2019 ETF→GP experiment, ADANN achieved an  $R^2$  of 0.73 and an RMSE of 1.15, far surpassing DANN, which recorded 0.56 and 1.47, respectively. These results indicate that ADANN more effectively reduces the feature distribution gap between source and target domains by leveraging adversarial learning and adaptive alignment strategies.

Furthermore, inter-annual environmental variability significantly affected model performance. For instance, abnormal wet conditions in parts of the Corn Belt in 2019 weakened the correlation between remote sensing features and actual yields, exacerbating domain discrepancies and degrading the performance of traditional models. Nonetheless, ADANN maintained stable and accurate predictions under such extreme conditions, demonstrating robust adaptability to real-world variations.

Overall, the four-year experimental results indicate that ADANN consistently performs well across both local and cross-domain settings. Its superior accuracy and lower error margins in domain transfer tasks underscore its suitability for cross-region yield modeling. While traditional models are effective in localized scenarios, they suffer substantial performance degradation under domain shifts. By contrast, ADANN emerges as a reliable solution for cross-domain agricultural remote sensing yield prediction, due to its stability, generalization capability, and adaptability.

To further investigate prediction bias, Figure 17 presents the spatial distribution of mean absolute errors from 2016 to 2019 for two domain adaptation scenarios: GP→ETF and ETF→GP. The results show that traditional models such

as RF and DNN exhibit significant error clustering in regions distant from the source domain, such as Michigan and Ohio. In contrast, adversarial learning-based models (DANN and ADANN) substantially reduce prediction errors in these regions. Notably, ADANN further mitigates spatial prediction bias in key agricultural zones like Illinois.

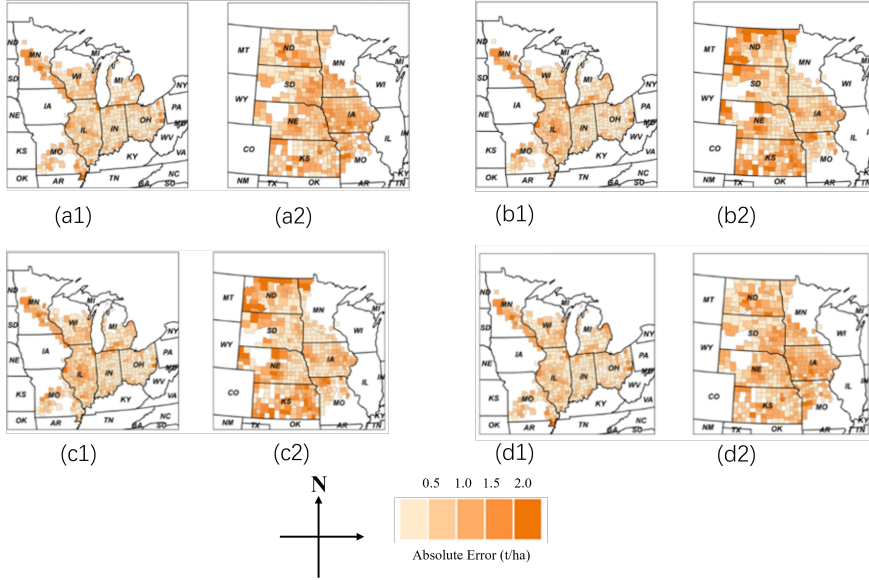


**Figure 17:** Mean absolute error maps from 2016 to 2019 for two domain adaptation experiments: (1) GP→ETF and (2) ETF→GP. Model types: (a1 a2) RF, (b1 b2) DNN, (c1 c2) DANN, and (d1 d2) ADANN. Image adapted from Ma et al. [141]

In summary, ADANN effectively extracts domain-invariant features through adversarial training, mitigating distribution discrepancies and reducing prediction bias. Its superior performance across four consecutive years in the U.S. Corn Belt validates its practicality and robustness. By maintaining a favorable balance between adversarial domain alignment and prediction accuracy, ADANN delivers stable and precise cross-domain yield predictions, setting a new benchmark for agricultural remote sensing modeling.

## 5.5. Remote Sensing-Based Agricultural Land Extraction Experiments

In the comparative experiment on agricultural land extraction from remote sensing imagery, we selected six representative domain adaptation methods for performance evaluation: a baseline model (trained solely on the source domain without adaptation), AdaptSegNet [102], ADVENT [103], BDL [104], IntraDA [67], and TransFusion-DualDA [86], as shown in Figure 18. The evaluation was conducted on three benchmark datasets (DeepGlobe, LoveDA, and GID), which differ significantly in spatial resolution and scene complexity.

Table 5 summarizes the quantitative results of the cross-domain experiments under three settings: DeepGlobe→LoveDA, GID→LoveDA, and DeepGlobe→GID. Across all transfer scenarios, TransFusion-DualDA consistently outperforms other methods, achieving the highest scores in key metrics such as IoU, COM, and F1. In the DeepGlobe→LoveDA setting, it achieves an IoU of 55.76% and an F1 score of 67.75%, surpassing IntraDA and BDL by 5–10 percentage points. This superior performance is attributed to its Transformer backbone’s capability for global context modeling and multi-scale feature fusion, which enables robust domain discrepancy handling.

In the GID→LoveDA setting, TransFusion-DualDA attains an exceptional COM of 92.11%, over 32% higher than the baseline. This result reflects its strong capacity to align spatial boundary structures, even when transferring from low-resolution (4 m/pixel) to ultra-high-resolution (0.3 m/pixel) imagery. Traditional methods struggle with such resolution disparities due to ineffective scale alignment.

In the DeepGlobe→GID scenario (high-to-low resolution), TransFusion-DualDA again outperforms its counterparts, achieving an F1 score of 62.44% and an IoU of 49.55%. Although the performance margins over IntraDA and BDL are narrower, the results highlight that limited resolution and reduced feature richness in GID constrain the transferability of high-resolution features. This suggests the need for models that better manage redundancy and preserve contextual semantics.



**Figure 18:** Sample images from three agricultural land datasets. (a) DeepGlobe (0.5 m/pixel); (b) LoveDA (0.3 m/pixel); (c) GID (4 m/pixel).

Figure 19 illustrates visual results for the DeepGlobe→GID task. The baseline (c) yields poor segmentation performance, exhibiting substantial confusion between farmland and background along with severe structural degradation. This demonstrates the ineffectiveness of directly applying source-domain models to target-domain data without adaptation.

With ADVENT (d) and IntraDA (e), segmentation quality improves. ADVENT employs adversarial learning to reduce domain gaps, while IntraDA introduces intra-class consistency constraints to enhance boundary smoothness. However, both methods still suffer from issues such as boundary blurring and region fragmentation.

TransFusion-DualDA (f) produces the most consistent and accurate segmentation results, with boundaries closely aligning to the ground truth and precise region-level predictions. Its advantage arises from effective long-range dependency modeling and all-scale feature fusion, enabling the simultaneous capture of fine details and global structure. Nevertheless, minor edge artifacts and residual noise remain, indicating opportunities for further enhancement in managing high-resolution image heterogeneity.

In conclusion, TransFusion-DualDA exhibits superior generalization across diverse spatial resolutions and land types. Its consistent advantages in COM and IoU metrics affirm its robustness for shape-preserving segmentation, making it a highly effective method for unsupervised domain adaptation in remote sensing-based agricultural land monitoring.

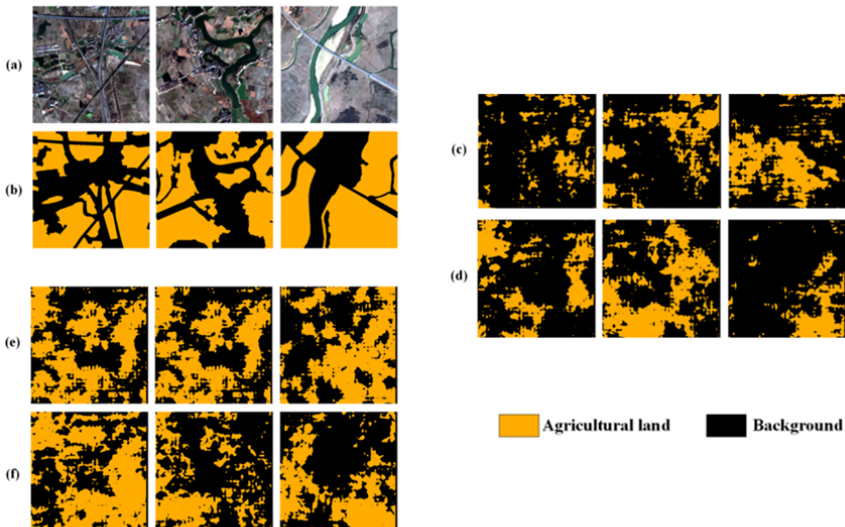
## 5.6. Summary of Experimental Findings

In the plant disease transfer detection task, MSUN achieves a leading average accuracy of 56.06%, substantially outperforming alternative methods such as DSAN (42.87%). It particularly excels in cross-domain classification

Source → Target	Method	IoU	COM	COR	F1
DeepGlobe → LoveDA	Source-only	36.327	45.895	62.861	49.108
	AdaptSegNet	46.921	74.478	55.190	60.404
	ADVENT	49.392	74.621	58.085	61.169
	BDL	52.234	79.747	59.011	65.334
	IntraDA	51.710	82.855	57.341	64.589
	TransFusion-DualIDA	<b>55.763</b>	<b>81.370</b>	<b>62.549</b>	<b>67.750</b>
GID → LoveDA	Source-only	36.229	40.139	83.018	46.026
	AdaptSegNet	42.931	54.221	71.295	55.454
	ADVENT	45.035	60.762	65.021	58.250
	BDL	44.592	58.231	67.447	57.732
	IntraDA	48.254	60.365	72.898	60.799
	TransFusion-DualIDA	<b>53.470</b>	<b>92.109</b>	56.891	<b>66.042</b>
DeepGlobe → GID	Source-only	26.986	39.204	62.884	36.599
	AdaptSegNet	43.098	68.614	59.414	56.067
	ADVENT	45.995	77.435	57.403	58.940
	BDL	46.348	75.789	58.373	59.508
	IntraDA	47.631	68.488	60.293	61.465
	TransFusion-DualIDA	<b>49.553</b>	<b>88.545</b>	54.535	<b>62.439</b>

**Table 5**

Performance comparison of domain adaptation methods across different dataset transfer settings.

**Figure 19:** Visualization of segmentation results under the DeepGlobe→GID setting. (a) Target image; (b) Ground truth; (c) Source-only; (d) ADVENT; (e) IntraDA; (f) TransFusion-DualIDA.

tasks involving corn, grape, sweet pepper, potato, and apple diseases, demonstrating strong adaptability to complex agricultural scenarios. Although MSUN’s accuracy on tomato disease classification is slightly lower (48.67%), models like DANN (49.51%) and MRAN (49.34%) provide potential baselines for further optimization. Notably, sweet pepper classification yields high accuracy across all methods (above 84%), likely due to its distinct morphological features.

The superior performance of MSUN can be attributed to its innovative architectural design. Multi-representation modules are employed to extract diverse features, thereby reducing both domain and category discrepancies. Sub-domain adaptation facilitates fine-grained semantic alignment, while uncertainty regularization effectively suppresses the noise introduced by pseudo-labels. These integrated mechanisms enable MSUN to achieve optimal results on

four public benchmark datasets, positioning it as a preferred solution for multi-crop disease diagnosis with enhanced generalization and accuracy.

In the crop yield prediction experiments across ecological regions of the U.S. Corn Belt, four models—RF, DNN, DANN, and ADANN—were evaluated. ADANN consistently achieves the highest predictive performance in both intra-domain and cross-domain scenarios from 2016 to 2019. For instance, in the 2019 local task ( $\text{GP} \rightarrow \text{GP}$ ), RF and DNN achieved  $R^2$  scores of 0.76 and 0.79 respectively, while ADANN improved upon this with an  $R^2$  of 0.85. In the cross-domain scenario ( $\text{GP} \rightarrow \text{ETF}$ ), RF and DNN saw sharp drops (0.49 and 0.30), whereas ADANN maintained a robust  $R^2$  of 0.63, significantly outperforming DANN (0.58).

Interpretability analysis reveals that ADANN effectively balances domain and prediction losses to mitigate the effects of domain shift. Spatial error analysis indicates that RF and DNN show pronounced error clustering in regions such as Michigan and Ohio. While DANN partially alleviates this issue through adversarial training, ADANN further reduces prediction errors in core agricultural zones like Illinois, underscoring its robustness under dynamic cross-regional shifts.

In the domain adaptation experiment for remote sensing-based agricultural land extraction, TransFusion-DualDA demonstrates clear superiority. In the DeepGlobe  $\rightarrow$  LoveDA setting, it achieves the highest IoU (55.763%) and F1-score (67.750%), outperforming ADVENT and AdaptSegNet by 6–7 percentage points. When migrating from low-resolution GID (4 m/pixel) to ultra-high-resolution LoveDA (0.3 m/pixel), TransFusion-DualDA achieves an IoU improvement of 5.2% and an F1-score gain of 6%, validating the effectiveness of its Transformer backbone and multi-scale feature fusion in modeling both global context and local structures.

In the reverse migration (DeepGlobe  $\rightarrow$  GID), despite the challenge of transferring from high- to low-resolution data, TransFusion-DualDA maintains competitive performance (F1 = 62.439%), outperforming conventional methods such as BDL. Qualitative results further demonstrate its superiority in boundary delineation and region completeness compared to ADVENT and IntraDA. However, some residual prediction noise persists in the target domain, underscoring the ongoing challenge of local feature alignment.

Overall, the experiments validate the effectiveness of domain-adversarial training and entropy-guided sub-domain partitioning in TransFusion-DualDA, particularly under cross-sensor and cross-region conditions. This approach significantly reduces reliance on manual annotations by narrowing the domain gap in complex environments such as urban-rural transitions. Future work will focus on enhancing global feature extraction in high-resolution scenes to improve adaptability in dynamic remote sensing applications.

## 6. Challenges and Future Research Directions

Current research in agricultural intelligence faces multifaceted challenges involving data complexity, methodological adaptability, and technological limitations. Although domain adaptation (DA) techniques have shown promise in addressing cross-domain issues—such as environmental heterogeneity and annotation scarcity—they continue to face significant bottlenecks in computational efficiency, interpretability, and generalizability under complex field scenarios. This section identifies key practical bottlenecks and proposes targeted research directions.

### 6.1. Model Adaptability Barriers in Field Scenarios

The deployment of deep models in real-world agricultural environments is hindered by the following core issues:

**1) Multi-scale spatiotemporal data fusion:** Significant resolution discrepancies exist across satellite (10–100 m/pixel), UAV (0.1–1 m/pixel), and ground-level (centimeter-scale) imagery. Existing 3D convolutional approaches struggle to effectively align features across such scales.

**2) Severe labeled data scarcity:** Field datasets often contain fewer than 50 samples per class, particularly for rare crop diseases. Conventional transfer learning approaches often experience performance degradation exceeding 30% when training samples fall below 100.

**3) Limitations in multimodal collaboration:** Hyperspectral imaging in field conditions is subject to radiometric fluctuations ( $\pm 30\%$  in light intensity), inducing distributional shifts over time. Such variance compromises the effectiveness of direct multimodal fusion strategies.

### 6.2. Key Future Research Directions

To address these challenges, we propose four critical research directions:

**(1) Lightweight Spatiotemporal Modeling Framework:** Design ultra-compact network architectures with fewer than 1M parameters, incorporating physical priors (e.g., crop growth models) to guide feature extraction. Emphasize spatiotemporal decoupling to enable effective cross-scale fusion between UAV (5 cm) and satellite (10 m) imagery. Target energy consumption should be reduced to 20% of current 3D CNN baselines.

**(2) Weakly Supervised Transfer Learning Paradigm:** Develop pseudo-labeling mechanisms leveraging the temporal continuity of crop growth stages to generate self-supervised signals. Implement curriculum learning guided by phenological patterns to achieve over 85% classification accuracy with fewer than 100 labeled samples.

**(3) Robust Multimodal Fusion System:** Design spectral normalization-based feature extractors to suppress illumination-induced noise. Introduce physically informed adversarial training to ensure cross-modality consistency under lighting variation of up to  $\pm 40\%$ . Establish sub-meter alignment protocols to address spatial inconsistencies between aerial and ground-level sensors.

**(4) Privacy-Preserving Collaborative Learning:** Enhance communication efficiency in federated learning frameworks to support daily updates within 10 Mbps bandwidth. Integrate differential privacy strategies compliant with GDPR, ensuring that performance degradation remains below 5% under a privacy budget of  $\epsilon = 2$ .

To facilitate real-world deployment, we recommend the construction of a standardized open benchmark that includes over 10 representative crops across three or more climate zones. This benchmark should incorporate realistic noise factors (e.g., device error  $\pm 5\%$ , occlusion rate 20%) to better align algorithmic development with practical robustness.

## 7. Conclusion

Despite recent advances, adaptive modeling in agriculture continues to face persistent challenges, particularly in addressing the complexity of spatiotemporal dynamics, annotation scarcity, and multimodal data heterogeneity. As agricultural environments become increasingly complex, the effectiveness of existing domain adaptation techniques—especially under cross-seasonal, cross-regional, and cross-modal scenarios—remains limited.

Future research should aim to develop task-specific, high-dimensional adaptive models to enhance performance in diverse agricultural applications such as crop health monitoring, yield prediction, and pest recognition. Unsupervised domain adaptation remains especially valuable in data-scarce scenarios, while multimodal fusion—including image, meteorological, and soil data—offers further potential to enhance model generalization. Moreover, source-free domain adaptation represents a critical research frontier, particularly when access to source data is restricted due to privacy or operational constraints.

Ultimately, the robustness of these models in field deployments depends on their ability to operate under unpredictable environmental conditions, across diverse crop types, and using heterogeneous sensor platforms. Overcoming these technical and operational barriers is essential to advance precision agriculture and intelligent farming. Enhancing model resilience and cross-domain adaptability will enable more accurate agricultural decision-making, yield forecasting, and disease monitoring, thus contributing to the sustainable transformation of modern agriculture.

## Acknowledgment

This project is jointly supported by the High-Quality Development Special Project of the Ministry of Industry and Information Technology (TC240A9ED-56), the Academician Workstation Program of Yunnan Province (202405AF140013), the Shanghai Agricultural Technology Innovation Project (2024-02-08-00-12-F00032), the Science and Technology Program of Qinghai Province (2024-NK-141S-4), and the Shanghai Municipal Commission of Science and Technology (Grant No. 24TS1415900).

## References

- [1] A. Zhang, Y. Yang, J. Xu, X. Cao, X. Zhen, and L. Shao, “Latent domain generation for unsupervised domain adaptation object counting,” *IEEE Transactions on Multimedia*, vol. 25, pp. 1773–1783, 2022.
- [2] J. Quiñonero-Candela, *Dataset shift in machine learning*. Mit Press, 2009.
- [3] R. N. Jogekar and N. Tiwari, “A review of deep learning techniques for identification and diagnosis of plant leaf disease,” *Smart Trends in Computing and Communications: Proceedings of SmartCom 2020*, pp. 435–441, 2020.
- [4] F. Dubourvieux, G. Lapouge, A. Loesch, B. Luvison, and R. Audigier, “Cumulative unsupervised multi-domain adaptation for holstein cattle re-identification,” *Artificial Intelligence in Agriculture*, vol. 10, pp. 46–60, 2023.
- [5] Y. Jiang and C. Li, “Convolutional neural networks for image-based high-throughput plant phenotyping: a review,” *Plant Phenomics*, 2020.

- [6] G. Csurka, "A comprehensive survey on domain adaptation for visual applications," *Domain adaptation in computer vision applications*, pp. 1–35, 2017.
- [7] M. Wang and W. Deng, "Deep visual domain adaptation: A survey," *Neurocomputing*, vol. 312, pp. 135–153, 2018.
- [8] G. Wilson and D. J. Cook, "A survey of unsupervised deep domain adaptation," *ACM Transactions on Intelligent Systems and Technology (TIST)*, vol. 11, no. 5, pp. 1–46, 2020.
- [9] W. M. Kouw and M. Loog, "A review of domain adaptation without target labels," *IEEE transactions on pattern analysis and machine intelligence*, vol. 43, no. 3, pp. 766–785, 2019.
- [10] V. M. Patel, R. Gopalan, R. Li, and R. Chellappa, "Visual domain adaptation: A survey of recent advances," *IEEE signal processing magazine*, vol. 32, no. 3, pp. 53–69, 2015.
- [11] S. Sun, H. Shi, and Y. Wu, "A survey of multi-source domain adaptation," *Information Fusion*, vol. 24, pp. 84–92, 2015.
- [12] S. Zhao, B. Li, P. Xu, and K. Keutzer, "Multi-source domain adaptation in the deep learning era: A systematic survey," *arXiv preprint arXiv:2002.12169*, 2020.
- [13] S. PanQ, "Yang, "a survey on transfer learning,"," *IEEE Trans. Knowl. Data Eng*, vol. 22, no. 10, pp. 1345–1359, 2010.
- [14] L. Shao, F. Zhu, and X. Li, "Transfer learning for visual categorization: A survey," *IEEE transactions on neural networks and learning systems*, vol. 26, no. 5, pp. 1019–1034, 2014.
- [15] J. Zhang, W. Li, P. Ogunbona, and D. Xu, "Recent advances in transfer learning for cross-dataset visual recognition: A problem-oriented perspective," *ACM Computing Surveys (CSUR)*, vol. 52, no. 1, pp. 1–38, 2019.
- [16] C. Tan, F. Sun, T. Kong, W. Zhang, C. Yang, and C. Liu, "A survey on deep transfer learning," in *Artificial Neural Networks and Machine Learning—ICANN 2018: 27th International Conference on Artificial Neural Networks, Rhodes, Greece, October 4–7, 2018, Proceedings, Part III 27*. Springer, 2018, pp. 270–279.
- [17] F. Zhuang, Z. Qi, K. Duan, D. Xi, Y. Zhu, H. Zhu, H. Xiong, and Q. He, "A comprehensive survey on transfer learning," *Proceedings of the IEEE*, vol. 109, no. 1, pp. 43–76, 2020.
- [18] R. Girshick, J. Donahue, T. Darrell, and J. Malik, "Rich feature hierarchies for accurate object detection and semantic segmentation," in *Proceedings of the IEEE conference on computer vision and pattern recognition*, 2014, pp. 580–587.
- [19] R. Girshick, "Fast r-cnn," in *Proceedings of the IEEE international conference on computer vision*, 2015, pp. 1440–1448.
- [20] R. Faster, "Towards real-time object detection with region proposal networks," *Advances in neural information processing systems*, vol. 9199, no. 10.5555, pp. 2969 239–2969 250, 2015.
- [21] A. Fuentes, S. Yoon, S. C. Kim, and D. S. Park, "A robust deep-learning-based detector for real-time tomato plant diseases and pests recognition," *Sensors*, vol. 17, no. 9, p. 2022, 2017.
- [22] M. Long, J. Wang, G. Ding, J. Sun, and P. S. Yu, "Transfer joint matching for unsupervised domain adaptation," in *Proceedings of the IEEE conference on computer vision and pattern recognition*, 2014, pp. 1410–1417.
- [23] M. A. Molina-Caballillas, M. J. Jiménez-Navarro, R. Arjona, F. Martínez-Álvarez, and G. Asencio-Cortés, "Diafan-tl: An instance weighting-based transfer learning algorithm with application to phenology forecasting," *Knowledge-Based Systems*, vol. 254, p. 109644, 2022.
- [24] C. Yaras, K. Kassaw, B. Huang, K. Bradbury, and J. M. Malof, "Randomized histogram matching: A simple augmentation for unsupervised domain adaptation in overhead imagery," *IEEE Journal of Selected Topics in Applied Earth Observations and Remote Sensing*, vol. 17, pp. 1988–1998, 2023.
- [25] Y. Cui, L. Wang, J. Su, S. Gao, and L. Wang, "Iterative weighted active transfer learning hyperspectral image classification," *Journal of Applied Remote Sensing*, vol. 15, no. 3, pp. 032 207–032 207, 2021.
- [26] H. Li, J. Li, Y. Zhao, M. Gong, Y. Zhang, and T. Liu, "Cost-sensitive self-paced learning with adaptive regularization for classification of image time series," *IEEE Journal of Selected Topics in Applied Earth Observations and Remote Sensing*, vol. 14, pp. 11 713–11 727, 2021.
- [27] D. Tuia, C. Persello, and L. Bruzzone, "Domain adaptation for the classification of remote sensing data: An overview of recent advances," *IEEE geoscience and remote sensing magazine*, vol. 4, no. 2, pp. 41–57, 2016.
- [28] M. Wang, D. Zhang, J. Huang, P.-T. Yap, D. Shen, and M. Liu, "Identifying autism spectrum disorder with multi-site fmri via low-rank domain adaptation," *IEEE Transactions on Medical Imaging*, vol. 39, no. 3, pp. 644–655, 2020.
- [29] B. Fernando, A. Habrard, M. Sebban, and T. Tuytelaars, "Unsupervised visual domain adaptation using subspace alignment," in *Proceedings of the IEEE international conference on computer vision*, 2013, pp. 2960–2967.
- [30] B. Sun, J. Feng, and K. Saenko, "Return of frustratingly easy domain adaptation," in *Proceedings of the Thirtieth AAAI Conference on Artificial Intelligence*, ser. AAAI'16. AAAI Press, 2016, p. 2058–2065.
- [31] J. Peng, W. Sun, T. Wei, and W. Fan, "A modified correlation alignment algorithm for the domain adaptation of gf-5 hyperspectral image," *Journal of Remote Sensing (Chinese)*, vol. 24, no. 4, pp. 417–426, 2020.
- [32] F. Weilandt, R. Behling, R. Goncalves, A. Madadi, L. Richter, T. Sanona, D. Spengler, and J. Welsch, "Early crop classification via multi-modal satellite data fusion and temporal attention," *Remote Sensing*, vol. 15, no. 3, p. 799, 2023.
- [33] J. Li, Y. Shen, and C. Yang, "An adversarial generative network for crop classification from remote sensing timeseries images," *Remote Sensing*, vol. 13, no. 1, p. 65, 2020.
- [34] Y. Wang, H. Huang, and R. State, "Cross domain early crop mapping with label spaces discrepancies using multicropgan," *ISPRS Annals of the Photogrammetry, Remote Sensing and Spatial Information Sciences*, vol. 10, pp. 241–248, 2024.
- [35] K. Takahashi, H. Madokoro, S. Yamamoto, Y. Nishimura, S. Nix, H. Woo, T. K. Saito, and K. Sato, "Domain adaptation for agricultural image recognition and segmentation using category maps," in *2021 21st International Conference on Control, Automation and Systems (ICCAS)*. IEEE, 2021, pp. 1680–1685.
- [36] L. Bruzzone and C. Persello, "A novel approach to the selection of spatially invariant features for the classification of hyperspectral images with improved generalization capability," *IEEE transactions on geoscience and remote sensing*, vol. 47, no. 9, pp. 3180–3191, 2009.
- [37] C. Persello and L. Bruzzone, "Kernel-based domain-invariant feature selection in hyperspectral images for transfer learning," *IEEE transactions on geoscience and remote sensing*, vol. 54, no. 5, pp. 2615–2626, 2015.

- [38] C. Paris and L. Bruzzone, "A sensor-driven hierarchical method for domain adaptation in classification of remote sensing images," *IEEE Transactions on Geoscience and Remote Sensing*, vol. 56, no. 3, pp. 1308–1324, 2017.
- [39] L. Yan, R. Zhu, Y. Liu, and N. Mo, "Tradaboost based on improved particle swarm optimization for cross-domain scene classification with limited samples," *IEEE Journal of Selected Topics in Applied Earth Observations and Remote Sensing*, vol. 11, no. 9, pp. 3235–3251, 2018.
- [40] Y. Tang and X. Li, "Set-based similarity learning in subspace for agricultural remote sensing classification," *Neurocomputing*, vol. 173, pp. 332–338, 2016.
- [41] B. Banerjee and S. Chaudhuri, "Hierarchical subspace learning based unsupervised domain adaptation for cross-domain classification of remote sensing images," *IEEE Journal of Selected Topics in Applied Earth Observations and Remote Sensing*, vol. 10, no. 11, pp. 5099–5109, 2017.
- [42] E. Aptoula and B. Yanikoglu, "Morphological features for leaf based plant recognition," in *2013 IEEE International Conference on Image Processing*. IEEE, 2013, pp. 1496–1499.
- [43] S. J. Pan, I. W. Tsang, J. T. Kwok, and Q. Yang, "Domain adaptation via transfer component analysis," *IEEE transactions on neural networks*, vol. 22, no. 2, pp. 199–210, 2010.
- [44] L. Bruzzone and D. F. Prieto, "Unsupervised retraining of a maximum likelihood classifier for the analysis of multitemporal remote sensing images," *IEEE Transactions on Geoscience and Remote Sensing*, vol. 39, no. 2, pp. 456–460, 2002.
- [45] ———, "A partially unsupervised cascade classifier for the analysis of multitemporal remote-sensing images," *Pattern Recognition Letters*, vol. 23, no. 9, pp. 1063–1071, 2002.
- [46] L. Bruzzone and R. Cossu, "A multiple-cascade-classifier system for a robust and partially unsupervised updating of land-cover maps," *IEEE Transactions on Geoscience and Remote Sensing*, vol. 40, no. 9, pp. 1984–1996, 2002.
- [47] L. Bruzzone, R. Cossu, and G. Vernazza, "Combining parametric and non-parametric algorithms for a partially unsupervised classification of multitemporal remote-sensing images," *Information Fusion*, vol. 3, no. 4, pp. 289–297, 2002.
- [48] S. Zhong and Y. Zhang, "An iterative training sample updating approach for domain adaptation in hyperspectral image classification," *IEEE Geoscience and Remote Sensing Letters*, vol. 18, no. 10, pp. 1821–1825, 2020.
- [49] H. Wei, L. Ma, Y. Liu, and Q. Du, "Combining multiple classifiers for domain adaptation of remote sensing image classification," *IEEE Journal of Selected Topics in Applied Earth Observations and Remote Sensing*, vol. 14, pp. 1832–1847, 2021.
- [50] J. Zhang, J. Liu, B. Pan, Z. Chen, X. Xu, and Z. Shi, "An open set domain adaptation algorithm via exploring transferability and discriminability for remote sensing image scene classification," *IEEE Transactions on Geoscience and Remote Sensing*, vol. 60, pp. 1–12, 2021.
- [51] S. Xu, X. Mu, D. Chai, and S. Wang, "Adapting remote sensing to new domain with elm parameter transfer," *IEEE Geoscience and Remote Sensing Letters*, vol. 14, no. 9, pp. 1618–1622, 2017.
- [52] S. Rajan, J. Ghosh, and M. M. Crawford, "Exploiting class hierarchies for knowledge transfer in hyperspectral data," *IEEE Transactions on Geoscience and Remote Sensing*, vol. 44, no. 11, pp. 3408–3417, 2006.
- [53] L. Bruzzone and M. Marconcini, "Domain adaptation problems: A dasvm classification technique and a circular validation strategy," *IEEE transactions on pattern analysis and machine intelligence*, vol. 32, no. 5, pp. 770–787, 2009.
- [54] C. Deng, X. Liu, C. Li, and D. Tao, "Active multi-kernel domain adaptation for hyperspectral image classification," *Pattern Recognition*, vol. 77, pp. 306–315, 2018.
- [55] I. Kalita, R. N. S. Kumar, and M. Roy, "Deep learning-based cross-sensor domain adaptation under active learning for land cover classification," *IEEE Geoscience and Remote Sensing Letters*, vol. 19, pp. 1–5, 2021.
- [56] A. Saboori, H. Ghassemian, and F. Razzazi, "Active multiple kernel fredholm learning for hyperspectral images classification," *IEEE Geoscience and Remote Sensing Letters*, vol. 18, no. 2, pp. 356–360, 2020.
- [57] E. Izquierdo-Verdiguier, V. Laparra, L. Gomez-Chova, and G. Camps-Valls, "Encoding invariances in remote sensing image classification with svm," *IEEE Geoscience and Remote Sensing Letters*, vol. 10, no. 5, pp. 981–985, 2012.
- [58] J. Wang, Y. Chen, H. Yu, M. Huang, and Q. Yang, "Easy transfer learning by exploiting intra-domain structures," in *2019 IEEE international conference on multimedia and expo (ICME)*. IEEE, 2019, pp. 1210–1215.
- [59] Y. Zhu, F. Zhuang, J. Wang, J. Chen, Z. Shi, W. Wu, and Q. He, "Multi-representation adaptation network for cross-domain image classification," *Neural Networks*, vol. 119, pp. 214–221, 2019.
- [60] B. Espejo-Garcia, N. Mylonas, L. Athanasakos, E. Vali, and S. Fountas, "Combining generative adversarial networks and agricultural transfer learning for weeds identification," vol. 204. Elsevier, 2021, pp. 79–89.
- [61] R. Lu, N. Wang, Y. Zhang, Y. Lin, W. Wu, and Z. Shi, "Extraction of agricultural fields via dasfnet with dual attention mechanism and multi-scale feature fusion in south xinjiang, china," *Remote Sensing*, vol. 14, no. 9, p. 2253, 2022.
- [62] Z. Li, S. Chen, X. Meng, R. Zhu, J. Lu, L. Cao, and P. Lu, "Full convolution neural network combined with contextual feature representation for cropland extraction from high-resolution remote sensing images," *Remote Sensing*, vol. 14, no. 9, p. 2157, 2022.
- [63] R. Shang, J. Zhang, L. Jiao, Y. Li, N. Marturi, and R. Stolk, "Multi-scale adaptive feature fusion network for semantic segmentation in remote sensing images," *Remote Sensing*, vol. 12, no. 5, p. 872, 2020.
- [64] X. Zhang, B. Cheng, J. Chen, and C. Liang, "High-resolution boundary refined convolutional neural network for automatic agricultural greenhouses extraction from gaofen-2 satellite imageries," *Remote Sensing*, vol. 13, no. 21, p. 4237, 2021.
- [65] M. Cordts, M. Omran, S. Ramos, T. Rehfeld, M. Enzweiler, R. Benenson, U. Franke, S. Roth, and B. Schiele, "The cityscapes dataset for semantic urban scene understanding," in *Proceedings of the IEEE conference on computer vision and pattern recognition*, 2016, pp. 3213–3223.
- [66] A. Ghanbari, G. H. Shirdel, and F. Maleki, "Semi-self-supervised domain adaptation: Developing deep learning models with limited annotated data for wheat head segmentation," *Algorithms*, vol. 17, no. 6, p. 267, 2024.
- [67] F. Pan, I. Shin, F. Rameau, S. Lee, and I. S. Kweon, "Unsupervised intra-domain adaptation for semantic segmentation through self-supervision," in *2020 IEEE/CVF Conference on Computer Vision and Pattern Recognition (CVPR)*, 2020, pp. 3763–3772.

- [68] V. Rani, S. T. Nabi, M. Kumar, A. Mittal, and K. Kumar, "Self-supervised learning: A succinct review," *Archives of Computational Methods in Engineering*, vol. 30, no. 4, pp. 2761–2775, 2023.
- [69] K. Najafian, L. Jin, H. R. Kutcher, M. Hladun, S. Horovatin, M. A. Oviedo-Ludena, S. M. P. De Andrade, L. Wang, and I. Stavness, "Detection of fusarium damaged kernels in wheat using deep semi-supervised learning on a novel wheatseedbelt dataset," in *Proceedings of the IEEE/CVF International Conference on Computer Vision*, 2023, pp. 660–669.
- [70] K. Najafian, A. Ghanbari, I. Stavness, L. Jin, G. H. Shirdel, and F. Maleki, "A semi-self-supervised learning approach for wheat head detection using extremely small number of labeled samples," in *Proceedings of the IEEE/CVF International Conference on Computer Vision*, 2021, pp. 1342–1351.
- [71] K. Najafian, A. Ghanbari, M. Sabet Kish, M. Eramian, G. H. Shirdel, I. Stavness, L. Jin, and F. Maleki, "Semi-self-supervised learning for semantic segmentation in images with dense patterns," *Plant Phenomics*, vol. 5, p. 0025, 2023.
- [72] L. Yang, H. Wenhui, Y. Huihuang, R. Yuan, W. Tan, J. Xiu, and Z. Jun, "Tomato detection method using domain adaptive learning for dense planting environments," vol. 40, no. 13, 2024.
- [73] Y. Zhu, F. Zhuang, J. Wang, G. Ke, J. Chen, J. Bian, H. Xiong, and Q. He, "Deep subdomain adaptation network for image classification," *IEEE transactions on neural networks and learning systems*, vol. 32, no. 4, pp. 1713–1722, 2020.
- [74] W. Teng, N. Wang, H. Shi, Y. Liu, and J. Wang, "Classifier-constrained deep adversarial domain adaptation for cross-domain semisupervised classification in remote sensing images," *IEEE Geoscience and Remote Sensing Letters*, vol. 17, no. 5, pp. 789–793, 2019.
- [75] X. Liu, X. Liu, B. Hu, W. Ji, F. Xing, J. Lu, J. You, C.-C. J. Kuo, G. El Fakhri, and J. Woo, "Suosis," in *Proceedings of the AAAI conference on artificial intelligence*, vol. 35, no. 3, 2021, pp. 2189–2197.
- [76] X. Liu, F. Xing, J. You, J. Lu, C.-C. J. Kuo, G. El Fakhri, and J. Woo, "Subtype-aware dynamic unsupervised domain adaptation," *IEEE Transactions on Neural Networks and Learning Systems*, vol. 35, no. 2, pp. 2820–2834, 2022.
- [77] X. Yang, L. Jiao, and Q. Pan, "Transfer adaptation learning for target recognition in sar images: A survey," *IEEE Journal of Selected Topics in Applied Earth Observations and Remote Sensing*, 2024.
- [78] I. J. Goodfellow, J. Pouget-Abadie, M. Mirza, B. Xu, D. Warde-Farley, S. Ozair, A. Courville, and Y. Bengio, "Generative adversarial nets," *Advances in neural information processing systems*, vol. 27, 2014.
- [79] Y. Ganin and V. Lempitsky, "Unsupervised domain adaptation by backpropagation," in *International conference on machine learning*. PMLR, 2015, pp. 1180–1189.
- [80] Y. LeCun, "The mnist database of handwritten digits," <http://yann.lecun.com/exdb/mnist/>, 1998.
- [81] F. Yu, A. Seff, Y. Zhang, S. Song, T. Funkhouser, and J. Xiao, "Lsun: Construction of a large-scale image dataset using deep learning with humans in the loop," *arXiv preprint arXiv:1506.03365*, 2015.
- [82] A. Krizhevsky, G. Hinton *et al.*, "Learning multiple layers of features from tiny images," 2009.
- [83] O. Russakovsky, J. Deng, H. Su, J. Krause, S. Satheesh, S. Ma, Z. Huang, A. Karpathy, A. Khosla, M. Bernstein *et al.*, "Imagenet large scale visual recognition challenge," *International journal of computer vision*, vol. 115, pp. 211–252, 2015.
- [84] P. Shamsolmoali, M. Zareapoor, H. Zhou, R. Wang, and J. Yang, "Road segmentation for remote sensing images using adversarial spatial pyramid networks," *IEEE Transactions on Geoscience and Remote Sensing*, vol. 59, no. 6, pp. 4673–4688, 2020.
- [85] G.-H. Kwak and N.-W. Park, "Unsupervised domain adaptation with adversarial self-training for crop classification using remote sensing images," *Remote Sensing*, vol. 14, no. 18, p. 4639, 2022.
- [86] J. Zhang, S. Xu, J. Sun, D. Ou, X. Wu, and M. Wang, "Unsupervised adversarial domain adaptation for agricultural land extraction of remote sensing images," *Remote Sensing*, vol. 14, no. 24, p. 6298, 2022.
- [87] S. Ji, D. Wang, and M. Luo, "Generative adversarial network-based full-space domain adaptation for land cover classification from multiple-source remote sensing images," *IEEE Transactions on Geoscience and Remote Sensing*, vol. 59, no. 5, pp. 3816–3828, 2020.
- [88] O. Tasar, Y. Tarabalka, A. Giros, P. Alliez, and S. Clerc, "Standardgan: Multi-source domain adaptation for semantic segmentation of very high resolution satellite images by data standardization," in *Proceedings of the IEEE/CVF Conference on Computer Vision and Pattern Recognition Workshops*, 2020, pp. 192–193.
- [89] D. Witich and F. Rottensteiner, "Appearance based deep domain adaptation for the classification of aerial images," *ISPRS Journal of Photogrammetry and Remote Sensing*, vol. 180, pp. 82–102, 2021.
- [90] W. Liu and F. Su, "A novel unsupervised adversarial domain adaptation network for remotely sensed scene classification," *International Journal of Remote Sensing*, vol. 41, no. 16, pp. 6099–6116, 2020.
- [91] L. Yan, B. Fan, H. Liu, C. Huo, S. Xiang, and C. Pan, "Triplet adversarial domain adaptation for pixel-level classification of vhr remote sensing images," *IEEE Transactions on Geoscience and Remote Sensing*, vol. 58, no. 5, pp. 3558–3573, 2019.
- [92] Y. Huang, J. Peng, N. Chen, W. Sun, Q. Du, K. Ren, and K. Huang, "Cross-scene wetland mapping on hyperspectral remote sensing images using adversarial domain adaptation network," *ISPRS Journal of Photogrammetry and Remote Sensing*, vol. 203, pp. 37–54, 2023.
- [93] M. B. Bejiga, F. Melgani, and P. Beraldini, "Domain adversarial neural networks for large-scale land cover classification," *Remote Sensing*, vol. 11, no. 10, p. 1153, 2019.
- [94] M. M. Al Rahhal, Y. Bazi, H. Al-Hwiti, H. Alhichri, and N. Alajlan, "Adversarial learning for knowledge adaptation from multiple remote sensing sources," *IEEE Geoscience and Remote Sensing Letters*, vol. 18, no. 8, pp. 1451–1455, 2020.
- [95] A. Elshamli, G. W. Taylor, A. Berg, and S. Areibi, "Domain adaptation using representation learning for the classification of remote sensing images," *IEEE Journal of Selected Topics in Applied Earth Observations and Remote Sensing*, vol. 10, no. 9, pp. 4198–4209, 2017.
- [96] M. Martini, V. Mazzia, A. Khalil, and M. Chiaberge, "Domain-adversarial training of self-attention-based networks for land cover classification using multi-temporal sentinel-2 satellite imagery," *Remote Sensing*, vol. 13, no. 13, p. 2564, 2021.
- [97] G. Mateo-García, V. Laparra, D. López-Puigdolers, and L. Gómez-Chova, "Cross-sensor adversarial domain adaptation of landsat-8 and proba-v images for cloud detection," *IEEE Journal of Selected Topics in Applied Earth Observations and Remote Sensing*, vol. 14, pp. 747–761, 2020.

- [98] L. Ma and J. Song, "Deep neural network-based domain adaptation for classification of remote sensing images," *Journal of Applied Remote Sensing*, vol. 11, no. 4, pp. 042612–042612, 2017.
- [99] L. Zhang, M. Lan, J. Zhang, and D. Tao, "Stagewise unsupervised domain adaptation with adversarial self-training for road segmentation of remote-sensing images," *IEEE Transactions on Geoscience and Remote Sensing*, vol. 60, pp. 1–13, 2021.
- [100] J. Guo, J. Yang, H. Yue, X. Liu, and K. Li, "Unsupervised domain-invariant feature learning for cloud detection of remote sensing images," *IEEE Transactions on Geoscience and Remote Sensing*, vol. 60, pp. 1–15, 2021.
- [101] J. Hoffman, D. Wang, F. Yu, and T. Darrell, "Fencs in the wild: Pixel-level adversarial and constraint-based adaptation," *arXiv preprint arXiv:1612.02649*, 2016.
- [102] Y.-H. Tsai, W.-C. Hung, S. Schulter, K. Sohn, M.-H. Yang, and M. Chandraker, "Learning to adapt structured output space for semantic segmentation," in *Proceedings of the IEEE conference on computer vision and pattern recognition*, 2018, pp. 7472–7481.
- [103] T.-H. Vu, H. Jain, M. Bucher, M. Cord, and P. Pérez, "Advent: Adversarial entropy minimization for domain adaptation in semantic segmentation," in *Proceedings of the IEEE/CVF conference on computer vision and pattern recognition*, 2019, pp. 2517–2526.
- [104] Y. Li, L. Yuan, and N. Vasconcelos, "Bidirectional learning for domain adaptation of semantic segmentation," in *Proceedings of the IEEE/CVF conference on computer vision and pattern recognition*, 2019, pp. 6936–6945.
- [105] X. Zhang, X. Yao, X. Feng, G. Cheng, and J. Han, "Dfenet for domain adaptation-based remote sensing scene classification," *IEEE Transactions on Geoscience and Remote Sensing*, vol. 60, pp. 1–11, 2021.
- [106] J. Zheng, W. Wu, S. Yuan, Y. Zhao, W. Li, L. Zhang, R. Dong, and H. Fu, "A two-stage adaptation network (tsan) for remote sensing scene classification in single-source-mixed-multiple-target domain adaptation ( $s^2m^2t$  da) scenarios," *IEEE Transactions on Geoscience and Remote Sensing*, vol. 60, pp. 1–13, 2021.
- [107] N. Makkar, L. Yang, and S. Prasad, "Adversarial learning based discriminative domain adaptation for geospatial image analysis," *IEEE Journal of Selected Topics in Applied Earth Observations and Remote Sensing*, vol. 15, pp. 150–162, 2021.
- [108] K. Saito, S. Yamamoto, Y. Ushiku, and T. Harada, "Open set domain adaptation by backpropagation," in *Proceedings of the European conference on computer vision (ECCV)*, 2018, pp. 153–168.
- [109] A. Farahani, S. Voghoei, K. Rasheed, and H. R. Arabnia, "A brief review of domain adaptation," *Advances in data science and information engineering: proceedings from ICDATA 2020 and IKE 2020*, pp. 877–894, 2021.
- [110] M. Long, Y. Cao, J. Wang, and M. Jordan, "Learning transferable features with deep adaptation networks," in *International conference on machine learning*. PMLR, 2015, pp. 97–105.
- [111] M. Baktashmotagh, M. T. Harandi, B. C. Lovell, and M. Salzmann, "Unsupervised domain adaptation by domain invariant projection," in *Proceedings of the IEEE international conference on computer vision*, 2013, pp. 769–776.
- [112] J. Shen, Y. Qu, W. Zhang, and Y. Yu, "Wasserstein distance guided representation learning for domain adaptation," in *Proceedings of the AAAI conference on artificial intelligence*, vol. 32, no. 1, 2018.
- [113] B. Sun and K. Saenko, "Deep coral: Correlation alignment for deep domain adaptation," in *Computer vision–ECCV 2016 workshops: Amsterdam, the Netherlands, October 8–10 and 15–16, 2016, proceedings, part III 14*. Springer, 2016, pp. 443–450.
- [114] A. dos Santos Ferreira, J. M. Junior, H. Pistori, F. Melgani, and W. N. Gonçalves, "Unsupervised domain adaptation using transformers for sugarcane rows and gaps detection," *Computers and Electronics in Agriculture*, vol. 203, p. 107480, 2022.
- [115] G. Guo, S. Lai, Q. Wu, Y. Shou, and W. Shi, "Enhancing domain adaptation for plant diseases detection through masked image consistency in multi-granularity alignment," *Expert Systems with Applications*, vol. 276, p. 127101, 2025.
- [116] J. Gao, W. Liao, D. Nuyttens, P. Lootens, W. Xue, E. Alexandersson, and J. Pieters, "Cross-domain transfer learning for weed segmentation and mapping in precision farming using ground and uav images," *Expert Systems with applications*, vol. 246, p. 122980, 2024.
- [117] R. Fu, J. Han, Y. Sun, S. Wang, M. A. Al-Absi, X. Wang, and H. Sun, "Robust crop disease detection using multi-domain data augmentation and isolated test-time adaptation," *Expert Systems with Applications*, p. 127324, 2025.
- [118] M. Long, H. Zhu, J. Wang, and M. I. Jordan, "Deep transfer learning with joint adaptation networks," in *International conference on machine learning*. PMLR, 2017, pp. 2208–2217.
- [119] Y. Zhu, F. Zhuang, J. Wang, J. Chen, Z. Shi, W. Wu, and Q. He, "Multi-representation adaptation network for cross-domain image classification," *Neural Networks*, vol. 119, pp. 214–221, 2019.
- [120] Y. Zhu, F. Zhuang, J. Wang, G. Ke, J. Chen, J. Bian, H. Xiong, and Q. He, "Deep subdomain adaptation network for image classification," *IEEE transactions on neural networks and learning systems*, vol. 32, no. 4, pp. 1713–1722, 2020.
- [121] S. Zhao, X. Yue, S. Zhang, B. Li, H. Zhao, B. Wu, R. Krishna, J. E. Gonzalez, A. L. Sangiovanni-Vincentelli, S. A. Seshia *et al.*, "A review of single-source deep unsupervised visual domain adaptation," *IEEE Transactions on Neural Networks and Learning Systems*, vol. 33, no. 2, pp. 473–493, 2020.
- [122] Q. Zhu, Y. Sun, Q. Guan, L. Wang, and W. Lin, "A weakly pseudo-supervised decorrelated subdomain adaptation framework for cross-domain land-use classification," *IEEE Transactions on Geoscience and Remote Sensing*, vol. 60, pp. 1–13, 2022.
- [123] Y. Li, Z. Cao, H. Lu, and W. Xu, "Unsupervised domain adaptation for in-field cotton boll status identification," *Computers and Electronics in Agriculture*, vol. 178, p. 105745, 2020.
- [124] A. S. Garea, D. B. Heras, and F. Argüello, "Tcanet for domain adaptation of hyperspectral images," *Remote Sensing*, vol. 11, no. 19, p. 2289, 2019.
- [125] Z. Li, X. Tang, W. Li, C. Wang, C. Liu, and J. He, "A two-stage deep domain adaptation method for hyperspectral image classification," *Remote Sensing*, vol. 12, no. 7, p. 1054, 2020.
- [126] Y. Zhang, W. Li, M. Zhang, Y. Qu, R. Tao, and H. Qi, "Topological structure and semantic information transfer network for cross-scene hyperspectral image classification," *IEEE Transactions on Neural Networks and Learning Systems*, 2021.
- [127] W. Wang, L. Ma, M. Chen, and Q. Du, "Joint correlation alignment-based graph neural network for domain adaptation of multitemporal hyperspectral remote sensing images," pp. 3170–3184, 2021.

- [128] X. Liang, Y. Zhang, and J. Zhang, "Attention multisource fusion-based deep few-shot learning for hyperspectral image classification," *IEEE Journal of Selected Topics in Applied Earth Observations and Remote Sensing*, vol. 14, pp. 8773–8788, 2021.
- [129] K. Yan, X. Guo, Z. Ji, and X. Zhou, "Deep transfer learning for cross-species plant disease diagnosis adapting mixed subdomains," *IEEE/ACM transactions on computational biology and bioinformatics*, vol. 20, no. 4, pp. 2555–2564, 2021.
- [130] A. Fuentes, S. Yoon, T. Kim, and D. S. Park, "Open set self and across domain adaptation for tomato disease recognition with deep learning techniques," *Frontiers in plant science*, vol. 12, p. 758027, 2021.
- [131] X. Wu, X. Fan, P. Luo, S. D. Choudhury, T. Tjahjadi, and C. Hu, "From laboratory to field: Unsupervised domain adaptation for plant disease recognition in the wild," *Plant Phenomics*, vol. 5, p. 0038, 2023.
- [132] E. Othman, Y. Bazi, F. Melgani, H. Alhichri, N. Alajlan, and M. Zuair, "Domain adaptation network for cross-scene classification," *IEEE Transactions on Geoscience and Remote Sensing*, vol. 55, no. 8, pp. 4441–4456, 2017.
- [133] X. Lu, T. Gong, and X. Zheng, "Multisource compensation network for remote sensing cross-domain scene classification," *IEEE Transactions on Geoscience and Remote Sensing*, vol. 58, no. 4, pp. 2504–2515, 2019.
- [134] S. Zhu, B. Du, L. Zhang, and X. Li, "Attention-based multiscale residual adaptation network for cross-scene classification," *IEEE Transactions on Geoscience and Remote Sensing*, vol. 60, pp. 1–15, 2021.
- [135] J. Geng, X. Deng, X. Ma, and W. Jiang, "Transfer learning for sar image classification via deep joint distribution adaptation networks," *IEEE Transactions on Geoscience and Remote Sensing*, vol. 58, no. 8, pp. 5377–5392, 2020.
- [136] T. J. Young, T. Z. Jubery, C. N. Carley, M. Carroll, S. Sarkar, A. K. Singh, A. Singh, and B. Ganapathysubramanian, "canopy fingerprints" for characterizing three-dimensional point cloud data of soybean canopies," *Frontiers in plant science*, vol. 14, p. 1141153, 2023.
- [137] R. Zhao, Y. Zhu, and Y. Li, "Cla: A self-supervised contrastive learning method for leaf disease identification with domain adaptation," *Computers and Electronics in Agriculture*, vol. 211, p. 107967, 2023.
- [138] S. P. Mohanty, D. P. Hughes, and M. Salathé, "Using deep learning for image-based plant disease detection," *Frontiers in plant science*, vol. 7, p. 215232, 2016.
- [139] D. Singh, N. Jain, P. Jain, P. Kayal, S. Kumawat, and N. Batra, "Plantdoc: A dataset for visual plant disease detection," in *Proceedings of the 7th ACM IKDD CoDS and 25th COMAD*, 2020, pp. 249–253.
- [140] R. Thapa, K. Zhang, N. Snavely, S. Belongie, and A. Khan, "The plant pathology challenge 2020 data set to classify foliar disease of apples," *Applications in plant sciences*, vol. 8, no. 9, p. e11390, 2020.
- [141] Y. Ma, Z. Zhang, H. L. Yang, and Z. Yang, "An adaptive adversarial domain adaptation approach for corn yield prediction," *Computers and Electronics in Agriculture*, vol. 187, p. 106314, 2021.